QUARTZ-SILLIMANITE KNOTS AND METAMORPHISM AT SOUTHERN INDIAN LAKE, MANITOBA

A Thesis

Submitted to the

Faculty of Graduate Studies and Research

The University of Manitoba

In Partial Fulfillment

of the Requirements for the Degree of

Master of Science

by

JOHN RONALD CRANSTONE

July, 1971

ABSTRACT

All outcrops in the area surrounding the northern portion of Southern Indian Lake were mapped during the summers of 1969 and 1970, and a report with accompanying geologic maps has been prepared for the Manitoba Mines Branch. Quartz-muscovite-microcline-plagioclase-sillimanite nodules occurring in five outcrops of Sickle-type metasediments were mapped and sampled in detail. Twenty thin sections were studied and six chemical analyses done.

The almost spherical knots are late or post tectonic, formed subsequent to two periods of folding. The metamorphic grade reached during the first period of folding (intense, isoclinal) is uncertain, however, extensive recrystallization occurred. The metamorphic grade reached during a second period of deformation (north-east trending) was the upper amphibolite facies of the low or medium (cordierite bearing) pressure facies series. Actual knot formation presumably was by simple metamorphic differentiation and segregation in beds of a suitable composition during increasing metamorphism or, less likely, was the result of potash realkalization of quartz-sillimanite knots formed in an earlier dealkalization event. Quartz muscovite knots occurring elsewhere in the Lynn Lake District appear to have formed at somewhat lower metamorphic grade.

TABLE OF CONTENTS

LIST OF TABLES

LIST OF ILLUSTRATIONS

INTRODUCTION

The thesis area (longitude 98°15', latitude 57°15') is situated on the eastern shore of Southern Indian Lake (Fig. 1).

Extensive drift-cover restricts rock outcrop to shoreline exposure.

Previous mapping in the locality was carried out on a reconnaissance scale by the Geological Survey of Canada (McInnes, 1913 and Quinn, 1959). During 1969 and 1970, the writer conducted a more comprehensive study of the area for the Province of Manitoba (Cranstone, 1971).

Sickle Group rocks in the Lynn Lake area (to the west of the area delineated in Fig. 1) have metamorphic assemblages which are non-diagnostic of metamorphic grade. Thus, the infrequent occurrence of quartz-muscovite-microcline-plagioclase-sillimanite knots in Sickle-type rocks in the map area is of considerable interest. Detailed mapping and sampling of one such outcrop (Fig. 2) was done in the hope of determining the precise metamorphic grade involved; the relationship of the nodules to the regional tectonic history; and possible origins of such nodules in the thesis locality, and elsewhere in the Lynn Lake area.

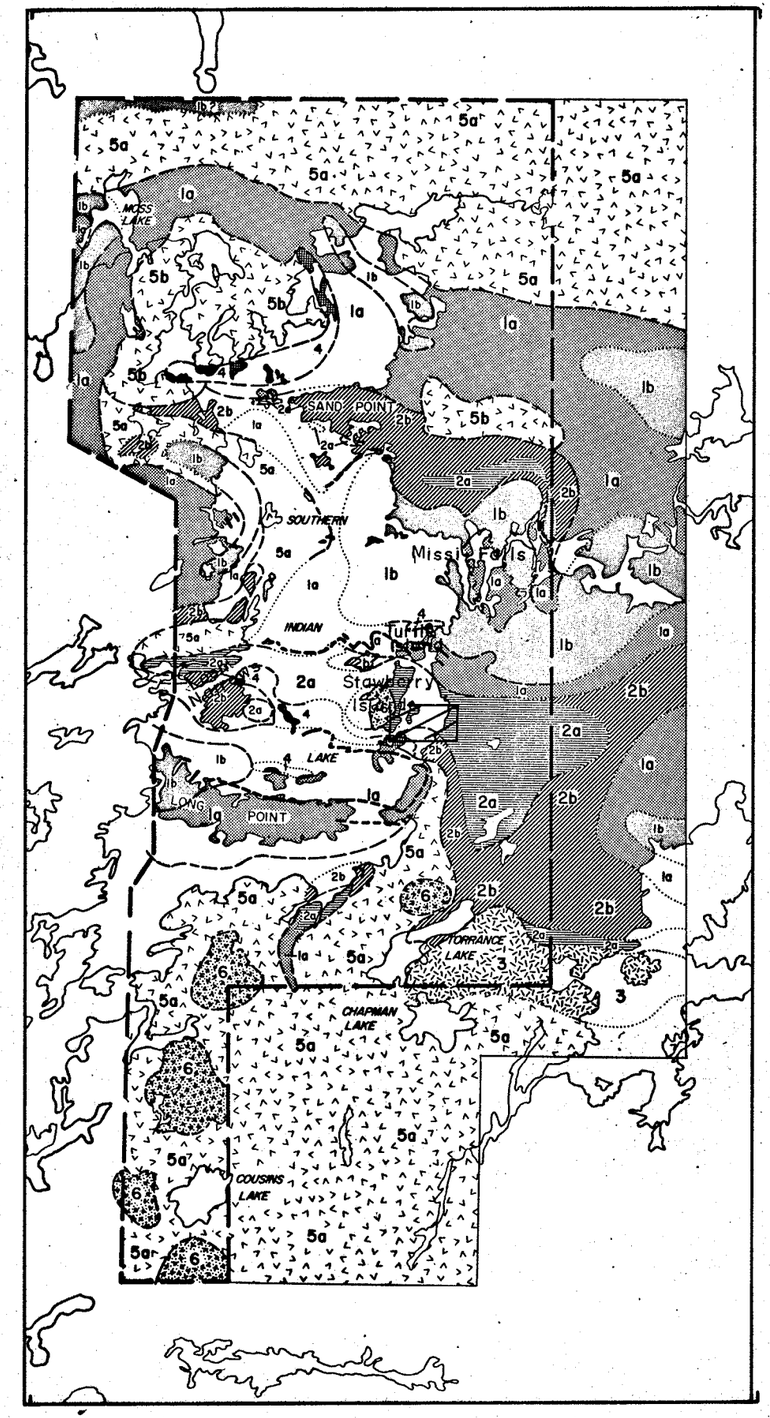

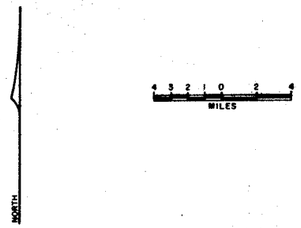

LEGEND

POST SICKLE INTRUSIVE ROCKS

- 6 Porphyritic - biotite quartz monzonite
- 5b Fine grained magnetite (hornblende - biotite) quartz monzonite
- 5a Porphyritic - hornblende quartz monzonite
- 4 Gabbro, diorite, quartz diorite, granodiorite (all genetically related)
- 3 Quartz diorite (perhaps pre - unit 2)

SICKLE GROUP ROCKS

- 2b Potassium feldspar metatexite, diatexite and anatectic quartz monzonite
- 2a Arkoses, conglomerates, sandstones, and derived layered gneisses

WASEKWAN GROUP ROCKS

- 1b Plagioclase diatexite, plagioclase anatexite
- 1a Plagioclase gneiss, plagioclase metatexite

Area of thesis study

MAP SYMBOLS

- Wasekwan calc-silicate horizon
- Approximate geological boundary
- Assumed geological boundary
- Fault
- Boundary of map area

Figure 1. Generalized geologic interpretation and correlation for the northern and eastern portions of Southern Indian Lake.

Data from geologic maps 6461, 6468, 6469, 6462(E), 6467E, 6410E, 6815E and figures of this report.

SOUTHERN

INDIAN

LAKE

DRIFT

DRIFT

DRIFT

DRIFT

LEGEND

78 — Foliation.

Bedding (tops known , tops unknown).

Geological boundary (defined, approximate , assumed , gradational).

Geological boundary with dip.

70 — Long axis of pebble stretch.

Shoreline.

T-7 — Station location.

Decreasing sillimanite knot occurrence

POST SICKLE INTRUSIVES

Pegmatite.

Meta-gabbro.

Porphyritic meta-gabbro. } BLACK TROUT DIORITE ?

SICKLE GROUP SEDIMENTS

Meta-sandstone ; meta-arkose.

Meta-conglomerate.

Index Map

98°45′ 98°00′ 57°45′ 57°00′ 56°45′

SCALE

0 10 20 30

FEET

Fig. 2 Detailed map of a typical sillimanite knot bearing outcrop

ACKNOWLEDGEMENTS

It is a pleasure to acknowledge the assistance of Mr. J. Bamburak, and Messrs. G. Beakhouse and M. Milinkovic in carrying out the detailed mapping.

Dr. A.C. Turnock of the University of Manitoba contributed valuable inspiration.

Chemical analyses were done by the Province of Manitoba Mines Branch Analytical Laboratory.

GENERAL GEOLOGY

The consolidated rocks of the Southern Indian Lake area are of Precambrian age and can be grouped into four subdivisions: Wasekwan-type rocks; Sickle-type rocks; post-Sickle-type basic intrusive rocks; post-Sickle-type granitic intrusive rocks (Fig. 1).

Wasekwan-type rocks consist mostly of migmatized, mobilized, potash deficient, "greywacke derived" gneisses and migmatites. These are overlain by Sickle-type psammites, variably mobilized or remobilized, often bedded, miogeosynclinally derived, potash-rich, granite pebble conglomerates arkoses and derived gneisses. The Sickle-type and Wasekwan-type rocks can be contrasted by differences in: preservation of primary features; aeromagnetic signature; grain size; mineralogic composition; relative degree of migmatization and mobilization; and complexity

of deformation. These differences are in keeping with the unconformable relationship between Wasekwan and Sickle rocks in the Lynn Lake area. Mineralized graphitic and calc-silicate marker horizons near the top of the Wasekwan-type rocks parallel the Sickle-Wasekwan contact. Small concordant calc-alkaline gabbro, diorite and hornblendite intrusions, followed by quartz monzonitic intrusive rocks of batholithic dimensions, intrude both Wasekwan and Sickle-type rocks.

The sequence described above closely resembles that reported by Milligan (1960) in the Lynn Lake - Granville Lake District. The terms "Wasekwan-type" and "Sickle-type" have been applied pending the establishment of a definite stratigraphic correlation with rocks of the Wasekwan and Sickle Groups.

Wasekwan and Sickle-type rocks contain mineral assemblages typical of the sillimanite-cordierite-muscovite and sillimanite-cordierite-amphibolite facies. The occurence of cordierite is restricted to Wasekwan-type rocks. The highly migmatitic nature of Wasekwan-type rocks relative to Sickle-type rocks may result from compositional differences between the two types rather than indicating pre-Sickle metamorphism. That the final metamorphic event was closely associated with widespread relatively shallow quartz monzonitic intrusion is indicated by the low pressure - high temperature metamorphic assemblages typical of the Abukuma-

type facies series.

Deformation in both Wasekwan-type and Sickle-type rocks consists of tight folding about a shallow easterly-plunging axis, followed by gentle cross-folding about an axis plunging moderately to the northeast. Quartz monzonitic intrusion was subsequent to east-west folding, and probably late syntectonic or post-tectonic to the northeast folding.

Mineralization consisting of disseminated pyrrhotite with small amounts of chalcopyrite and infrequently molybdenite is rare and appears to be pre-metamorphic, probably primary, and confined to graphitic horizons in Wasekwan-type rocks near the Sickle-Wasekwan contact.

TECTONIC ENVIRONMENT OF KNOT FORMATION

A detailed tectonic history of the area is given by Cranstone, 1971.

The most common form of quartz-muscovite-microcline-plagioclase-sillimanite knots in the Sickle-type rocks is spherical, in contrast to the highly-stretched pebbles in the host conglomerates. This indicates that nodules were formed subsequent to the initial, intense, isoclinal deformation. Also, the parallelism between muscovite alignment in the nodules, and the weak, northeast muscovite cross-foliation suggests that nodule formation was late-syntectonic to the northeast folding. A few knots showing elongation had a wide range in azimuth and plunge, with an average shallow northeast plunge.

Sillimanite-muscovite knots (compare this simple two mineral assemblage to the complex five mineral Sickle-assemblage) in the Wasekwan-type rocks are smaller, highly-stretched and finer-grained than those in Sickle-type rocks. Such growths in Wasekwan-type frequently have long axes closer to the early easterly-plunging axes of folding, and thus appear to be pre-Sickle in origin.

METAMORPHISM

General

The observed mineral assemblages are as follows (minerals in each assemblage are listed in their approximate order of relative abundance):

Wasekwan paragneisses and migmatites

(1) Plagioclase-quartz-biotite

(2) Plagioclase-quartz-biotite-garnet

(3) Plagioclase-quartz-biotite-microcline±garnet

(4) Plagioclase-quartz-biotite-microcline-muscovite±garnet

(5) Plagioclase-quartz-biotite-muscovite

(6) Plagioclase-quartz-sillimanite-biotite±garnet±microcline ±muscovite

(7) Plagioclase-quartz-hornblende-biotite

(8) Plagioclase-quartz-biotite-garnet-anthophyllite-muscovite

(9) Plagioclase-quartz-biotite-sillimanite-orthoclase

(10) Plagioclase-quartz-biotite-cordierite

(11) Plagioclase-quartz-biotite-cordierite-garnet

(12) Plagioclase-quartz-biotite-cordierite-sillimanite-microcline±muscovite

Wasekwan meta-calcareous rocks

(13) Plagioclase-quartz-diopside

(14) Hornblende-plagioclase-quartz-diopside-garnet-(ilmenite?)-magnetite-graphite-pyrrhotite

(15) Hornblende-diopside-plagioclase-ilmenite-magnetite-graphite-pyrrhotite

Sickle-type potassium feldspar-bearing rocks

(16) Plagioclase-quartz-microcline-biotite±magnetite

(17) Plagioclase-quartz-microcline-biotite-muscovite ±magnetite

(18) Plagioclase-quartz-microcline-biotite-muscovite-hornblende-magnetite±epidote

(19) Plagioclase-quartz-microcline-apatite-magnetite

(20) Plagioclase-quartz-sillimanite-microcline-biotite-muscovite-magnetite

Sickle-type plagioclase gneisses and migmatites

(21) Plagioclase-quartz-biotite-magnetite±garnet

(22) Plagioclase-quartz-biotite-microcline

(23) Plagioclase-quartz-sillimanite-muscovite

Sillimanite-muscovite and sillimanite-orthoclase-bearing assemblages typical of the amphibolite facies of Turner and Verhoogen (1960) and Winkler (1967) are widespread but not common. Cordierite, often associated with sillimanite, muscovite and/or orthoclase, occurs in the same widespread sporadic manner. Winkler (1967) states that

cordierite is never encountered in his Barrovian facies or in the almandine-amphibolite facies of Turner and Verhoogen (1960), rather, cordierite is characteristic of low pressure, Abukuma-type, cordierite-amphibolite facies. Table I shows the relationships of the various amphibolite facies as well as indicating the critical assemblages for the two subfacies found in the map-area. The widely-scattered, persistent occurrence of cordierite in Wasekwan rocks throughout the area (Fig. 1) suggests that low pressures were universal.

Figures 3, 4, and 5 are ACF and AKF diagrams for subfacies of the cordierite amphibolite facies after Winkler (1967). They suggest that the following subfacies may be, or may have been, present in the map-area:

(1) Sillimanite-cordierite-orthoclase-almandine subfacies
(2) Sillimanite-cordierite-muscovite subfacies
(3) Andalusite-cordierite-muscovite subfacies

Assemblages in which sillimanite-orthoclase± cordierite co-exist are restricted to Wasekwan-type plagioclase diatexites northwest of Missi Falls (Fig. 1).

Plagioclase metatexites on, and near, Long Point and near Missi Falls contain co-existing sillimanite, microcline and muscovite±cordierite, and thus are characteristic of the cordierite-sillimanite-muscovite subfacies.

Quartz-sillimanite-muscovite-microcline-plagioclase

Table I

Critical minerals or mineral associations of the subfacies of the amphibolite facies in different facies series (after Winkler, 1967). Mineral associations blocked in are critical assemblages present in the Southern Indian Lake area.

The amphibolite facies begins at approximately the same temperature in each facies series. The amphibolite facies has been subdivided on the basis of the upper stability of staurolite in the common parageneses and the upper stability of muscovite in the presence of quartz. These limits are indicated by the third and fourth solid horizontal lines, respectively. The horizontal dashed line represents the transition from andalusite to sillimanite.

Increasing P ⟶

Increasing T ⟶

Hornfels facies	Central Pyrenees (Bosost)	Abukuma-type	Eastern Pyrenees	Northern New Hampshire	Barrovian-type
staurolite; andalusite + cordierite + muscovite	staurolite; andalusite + cordierite + muscovite	staurolite; andalusite + cordierite + muscovite	staurolite; andalusite + almandine; cordierite	staurolite; andalusite + almandine	staurolite; kyanite + almandine
				staurolite; sillimanite + almandine	
andalusite + cordierite + muscovite	andalusite + cordierite + muscovite	andalusite + cordierite + muscovite	andalusite + almandine + muscovite	sillimanite + almandine + muscovite	kyanite + almandine + muscovite
	sillimanite + cordierite + muscovite	sillimanite + cordierite + Mn-bearing almandine + muscovite	sillimanite + almandine + muscovite		
at first andalusite, then sillimanite + cordierite + orthoclase	sillimanite + cordierite + orthoclase*	sillimanite + cordierite + almandine + orthoclase	sillimanite + almandine + orthoclase	sillimanite + almandine + orthoclase*	sillimanite + almandine + orthoclase

*At the present level of erosion, this subfacies is not exposed; however, it is to be expected at greater depths. In other similar metamorphic tracts, this subfacies has been reported.

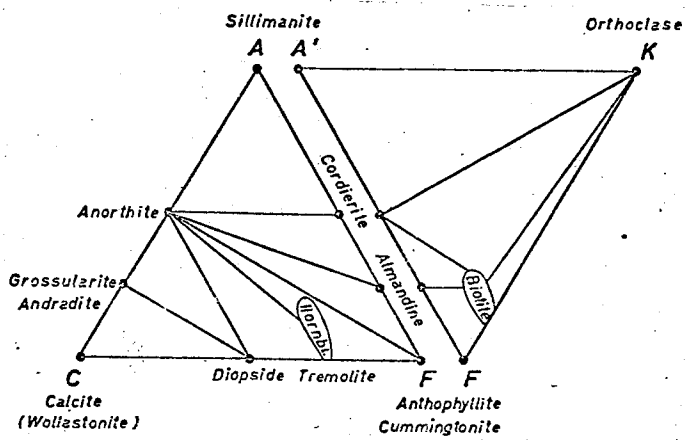

Fig. 3. Sillimanite-cordierite-orthoclase-almandine subfacies of the cordierite-amphibolite facies Biotite may co-exist with willimanite (after Winkler, 1967).

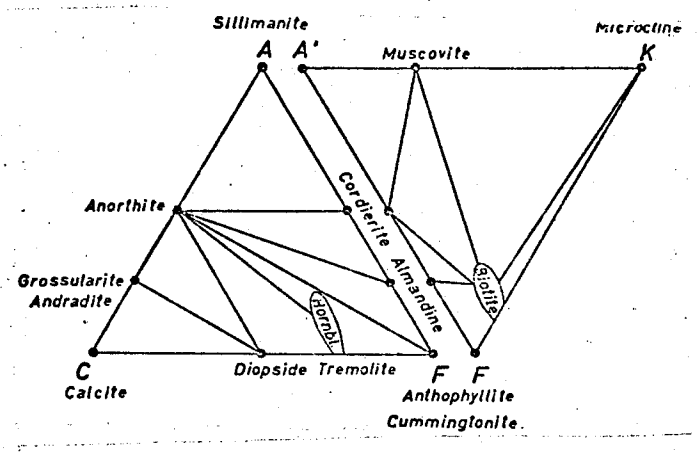

Fig. 4. Sillimanite-cordierite-muscovite-almandine subfacies of the cordierite-amphibolite facies of the Abukuma-type metamorphism. Biotite may co-exist with sillimanite. It is shown here that cordierite + almandine co-exist with biotite but not with muscovite.

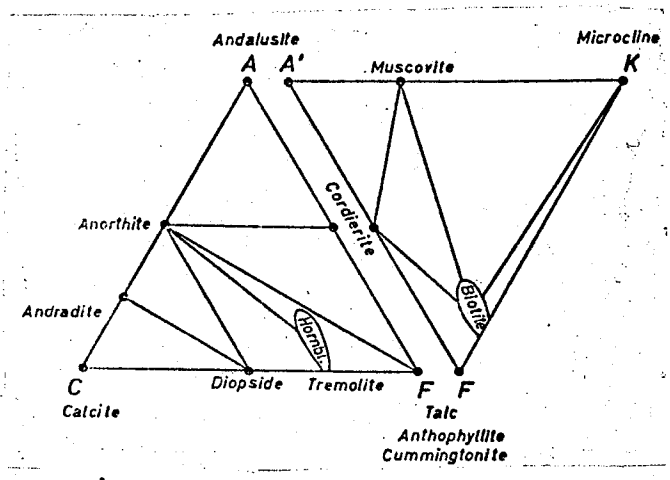

Fig. 5. Andalusite-cordierite-muscovite subfacies of the cordierite-amphibolite facies of the Abukuma-type metamorphism. Proper bulk chemical composition forthcoming, staurolite is also to be expected. In this case, and if muscovite is present, staurolite plots at the same place as cordierite. Biotite may co-exist with andalusite (after Winkler, 1967).

knots occur in Sickle Group metasediments in the area around Strawberry Island, and sillimanite-muscovite knots in Wasekwan plagioclase paragneisses, on and near Turtle Island and below Missi Rapids (Fig. 1).

The presence of quartz, sillimanite, K-feldspar and muscovite in near grain to grain contact and rarely in actual contact suggest that these knots represent the reaction:

$$KAl_2AlSi_3O_{10}(OH)_2 + SiO_2 \rightarrow Al_2SiO_5 + KAlSi_3O_8 + H_2O \quad (1)$$

muscovite — quartz — sillimanite — K-feldspar — water

Similar quartz-muscovite-sillimanite knots, usually devoid of K-feldspar, have been found in Sickle Group rocks elsewhere, especially in the Lynn Lake area by Milligan (1960), Barry (1965) and D.A. Cranstone (1968). These knots have variously been attributed to prograde and retrograde metamorphism.

The area of Sickle rocks, north of Loon Narrows (Fig. 1) is completely lacking in sillimanite-bearing assemblages. Diopside, indicative of the amphibolite facies, is the only indicator mineral present. Rocks in this area may lack suitable composition for the formation of sillimanite, or they may be of lower metamorphic grade. Thus, although andalusite has not been found, the possibility of it's being stable (as per Fig. 5) should be considered.

Temperature and Pressure of Metamorphism

According to Winkler (1967), pressure and temperatures operating during Abukuma-type metamorphism are:

(1) Cordierite-sillimanite-muscovite subfacies, 3000 bars, 630°-670°C.

(2) Cordierite-sillimanite-orthoclase-almandine subfacies, 3000-3500 bars, 670°-720°C.

Figure 6 is Winkler's (1967) synthesis of mineral stability data, onto which has been plotted Richardson's (1968) experimental iron cordierite stability range. These curves may shift somewhat with variation in O_2 and H_2O partial pressures, and with cordierite Fe/Mg ratios. Staurolite is not found in the area, and orthopyroxene (hypersthene) was only observed at one location (on Long Point, Fig. 1). Since the hypersthene lacks retrograde textures, it has been taken as being formed during prograde metamorphism between the upper amphibolite and granulite facies. The possibility of the hypersthene being relict from a previous metamorphic event should, however, be considered in light of the probable multiple metamorphic history of the area. Temperature-pressure ranges must have reached within the patterned range in Fig. 6 during the thermal culmination of the last phase of metamorphism. These ranges are 1.5-4.5 kilobars, and 640°-760°C. Cordierite-bearing assemblages are restricted to pressures of 3.2 kilobars or less, although stability at somewhat higher

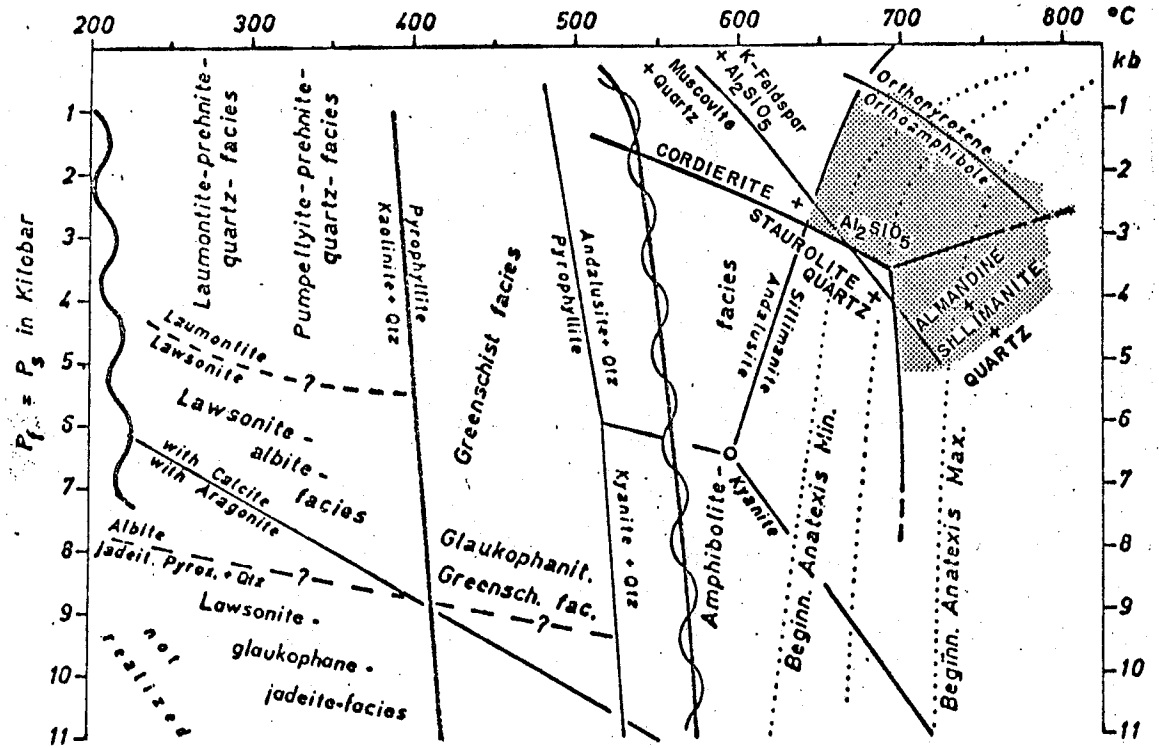

Fig. 6. Pressure and temperature conditions of metamorphism (after Winkler, 1967). Cordierite stability fields from Richardson (1968). Patterned field represents metamorphic mineral assemblages found in the Southern Indian Lake area.

pressures might be expected for Mg-rich cordierite.

Figure 7 shows stability fields for kyanite, andalusite and sillimanite as given by Newton (1966). Superimposed on Newton's diagram are Richardson's (1968) iron-cordierite stability curves, the granite solidus curve of Tuttle and Bowen (1958), Winkler's (1966) greywacke solidus curve for muscovite-quartz-K-feldspar-sillimanite (and/or andalusite). The diagram reveals that assemblages present in the map area could have developed at between 600° and 800°C, over a range of pressures. However, the widespread existence of cordierite-bearing assemblages in rocks of suitable chemical composition restricts these pressures to less than 3.5 kilobars. Slightly higher pressures might be expected with increasing Mg percentage in cordierite.

Widespread areas of anatexis, outlined in Fig. 8 are present in both Sickle and Wasekwan-type rocks. The general chemical composition of Sickle-type rocks is similar to that of quartz monzonites, whereas Wasekwan-type rocks have compositions similar to greywackes. Solidus curves proposed by Tuttle and Bowen (1958) and Winkler (1966)(Figs. 6 and 7) indicate that melting temperatures for these rocks at 2-4 kilobars pressure are between 675° and 710°C.

Figure 9 (in pocket) shows a ternary projection of the cotectic line of the system: SiO_2 - $NaAlSi_3O_8$ - $KAlSi_3O_8$ - H_2O at pH_2O = 2000 bars. Ternary plots of quartz + plagioclase

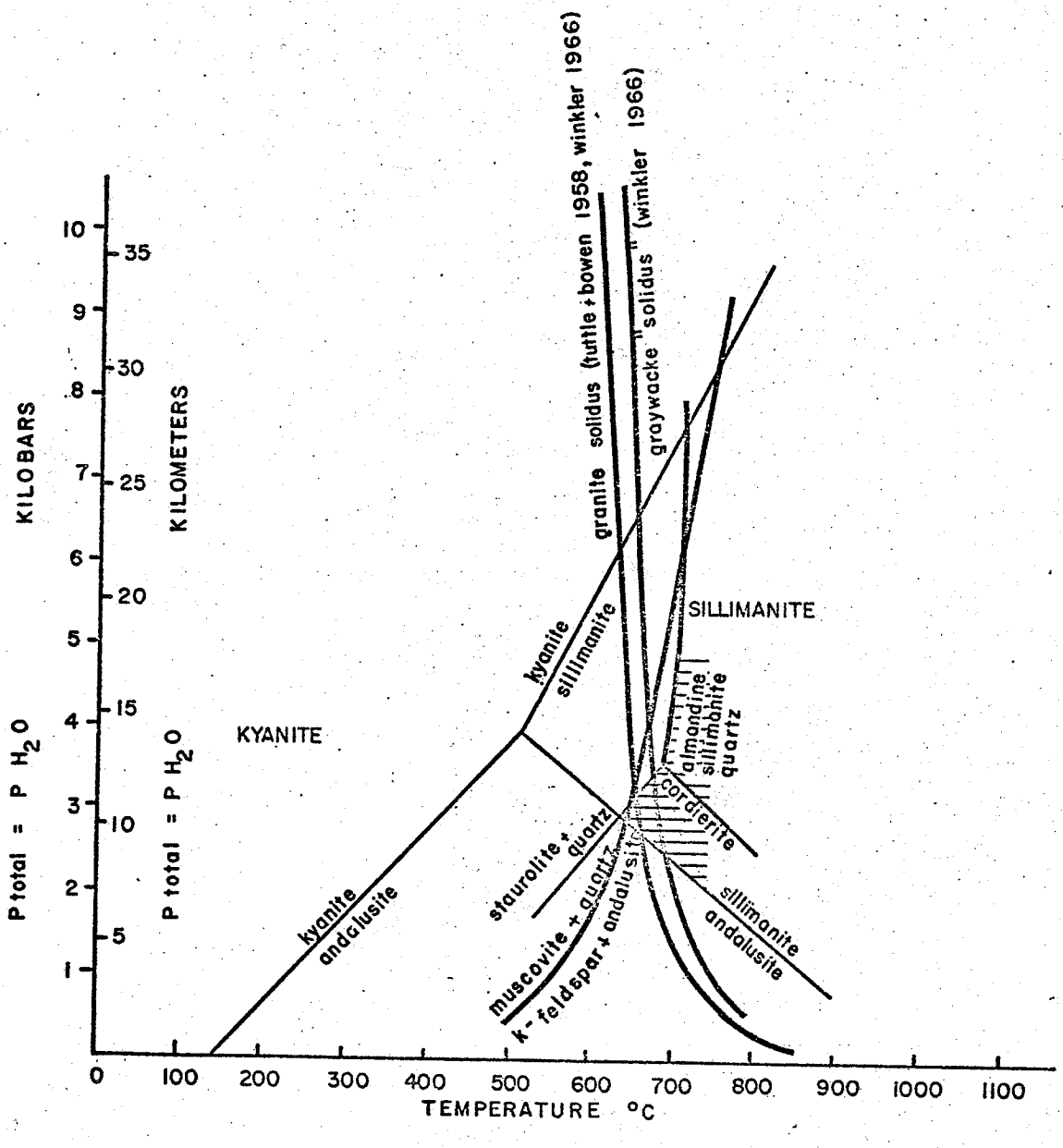

Fig. 7. Stability fields for kyanite, andalusite and sillimanite, after Newton (1966), and cordierite stability field from Richardson (1968). Patterned field represents metamorphic assemblages found in the Southern Indian Lake area.

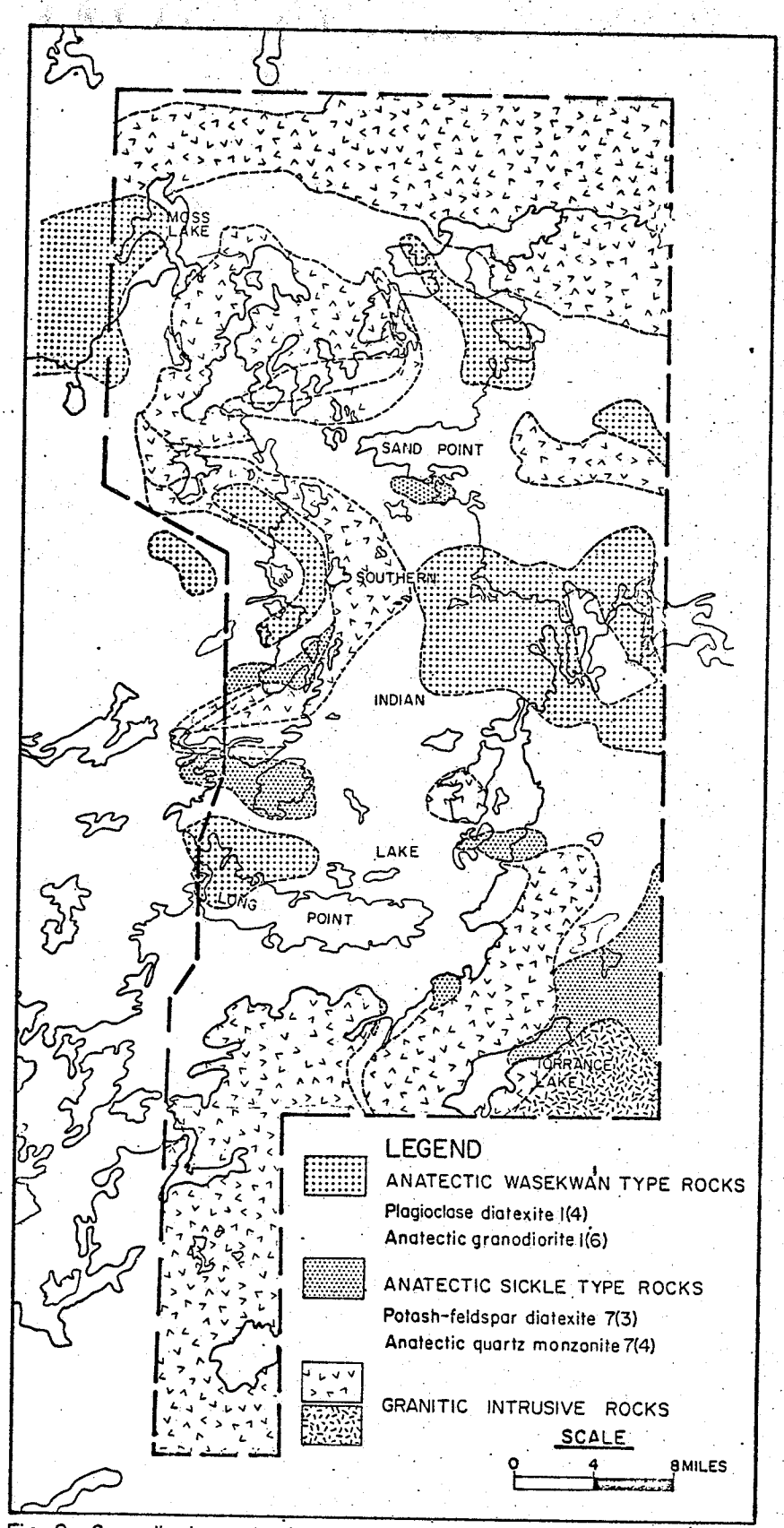

Fig. 8 Generalized map showing areas of extreme anatexis for Wasekwan and Sickle type rocks.

+ feldspar for all rock units can be compared to this diagram to determine the temperature required for anatexis to begin in each. Compositions of Sickle-type rocks lie in, or near, the minimum melting region 680° - 725°C, while Wasekwan-type rocks generally lie in the 725° - 800°C melting region. This distribution may explain the highly migmatitic nature of Wasekwan-type rocks relative to Sickle-type rocks. The composition of a large portion of the Sickle-type rocks lies in the minimum melting zone, resulting in pervasive or en-masse melting to yield a homogeneous non-migmatitic rock. However, Wasekwan-type rocks, and some Sickle-type rocks which fall outside this minimum melting zone may form migmatites in lit-par-lit fashion. Thus, the relatively migmatitic nature of Wasekwan-type rocks should not be used as a criteria for a pre-Sickle metamorphic event.

Both Wasekwan and Sickle-type rocks appear to have undergone the same degree and type of metamorphism and no textural evidence was found to indicate pre-Sickle metamorphism, although the possibility of complete overprinting by a post-Sickle event is quite likely. One could imply that the relatively low-pressure environment of metamorphism (2-4 kilobars) indicates relatively shallow burial and thereby a high geothermal gradient. The logical source of heat would be the batholithic bodies of late-kinematic porphyritic hornblende-quartz monzonite.

QUARTZ-SILLIMANITE KNOTS

Outcrop Description

Bands containing somewhat elliptical to spherical quartz-muscovite-microcline-plagioclase-sillimanite knots occur in interbedded Sickle-type psamites (metamorphosed conglomerates, arkoses, and sandstones). The spherical undeformed nature of these knots contrasts with the large degree of stretching of the pebbles in the conglomerates, which measure from 1:2:10 to 1:1:20. Figures 10 and 11 give an indication of the control exerted by primary layering on knot distribution and frequency. Knots are mostly confined to specific horizons and/or lenses, particularly lenticular bands of arkose in conglomerate as delineated in Fig. 2.

Figure 12 shows typical knots, size 1 x ½ inches, present in the conglomerate-arkose, while Fig. 13 indicates extremely large knots, 3 x 3 inches, found in highly mobilized, anatectic, derivatives of the conglomerate arkose. In general, knot size increases with the "bulk melting" characteristic of Sickle-type rocks. This correlation is described in the preceding section pertaining to metamorphic setting.

Potash feldspar-bearing pebbles in the conglomerate

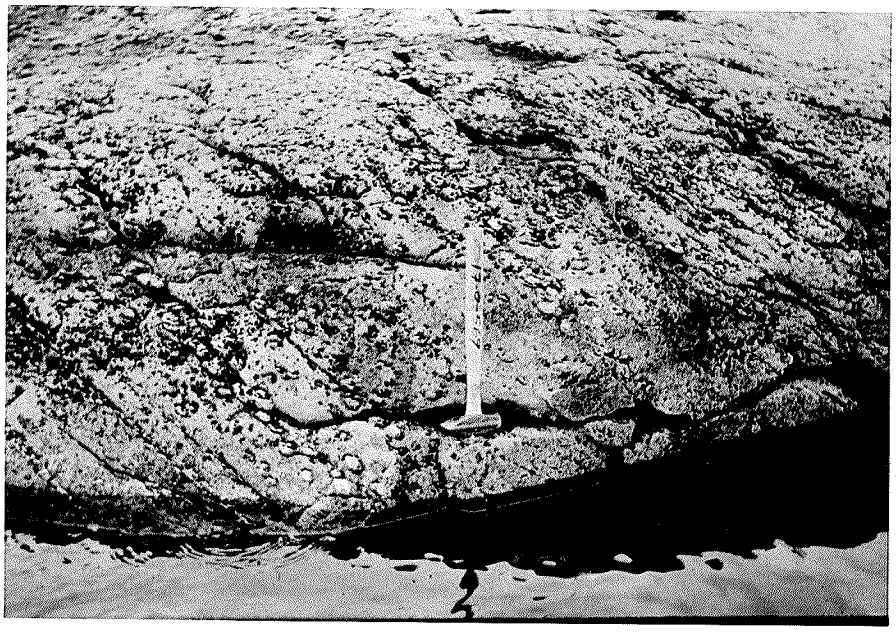

Fig. 10. Knots following layering in Sickle-type potash-feldspar gneiss. Strawberry Island.

Fig. 11. Knots in layering of potash-feldspar gneiss. Note somewhat-elliptical form of knots. Strawberry Island.

Fig. 12. Typical knots in interbedded conglomerate-arkose. On lakeshore east of Strawberry Island.

Fig. 13. Large nodules in homogeneous, Sickle-type potash-feldspar diatexite. Strawberry Island.

are observed, rarely, to provide a nucleus for knot formation.

In hand specimen the nodules appear to contain a leucocratic, coarse-grained, quartz and muscovite rich core which is surrounded by a microcline and quartz rich rim. Knots are set in a weakly foliated, fine-grained, pink-white weathering matrix consisting of quartz, potash feldspar, plagioclase, biotite and muscovite. An extremely weak, northeast, cross foliation is infrequently present in the matrix. A darker, 1/8 inch wide halo, enriched in biotite, is common in the matrix immediately in contact with the nodules.

Thin Section Description

In thin section, the knots consist of 30-50 percent coarse, bladed, poikiloblastic muscovite and 30-50 percent quartz. Microcline and lesser sillimanite and apatite constitute less than 20 percent of the knot (Table II). Sillimanite typically occurs as microscopic needles in quartz (Fig. 14), and less commonly in muscovite and microcline (Figs. 15a and 15b). Sillimanite does, however, occasionally occur in sheafs. The microcline content of the knots is characteristically considerably lower than in the surrounding matrix (see Table II). A 1/8 inch wide, microcline-rich rim is commonly evident on the knots; these rims are commonly accompanied by microcline and biotite

Table II

A. Mineralogical content of nodules (5 samples)

	Average	Range
Plagioclase (An=20)	7%	4-10%
Microcline	7	5-10
Quartz	39	37-41
Biotite	2	1-2
Muscovite	43	40-45
Magnetite	2	1-2

B. Mineralogical compositions of matrix (7 samples)

	Average	Range
Plagioclase (An=20)	21%	16-27%
Microcline	24	15-32
Quartz	42	39-43
Biotite	8	6-20
Muscovite	5	2-10
Magnetite	3	3-4

Fig. 14. Sillimanite needles in quartz surrounded by muscovite in typical knot. Muscovite invagination into quartz (centre) appears to be after sillimanite. Crossed polars.

Fig. 15a. Sillimanite in quartz, and microcline in close proximity to muscovite, in one of the knots. Note poikilitic quartz in microcline. Crossed polars.

Fig. 15b. Sillimanite in quartz, and microcline in close proximity to muscovite, in one of the knots. Crossed polars.

Fig. 15c. Poikiloblastic texture in typical knot with microcline surrounding quartz. Crossed polars.

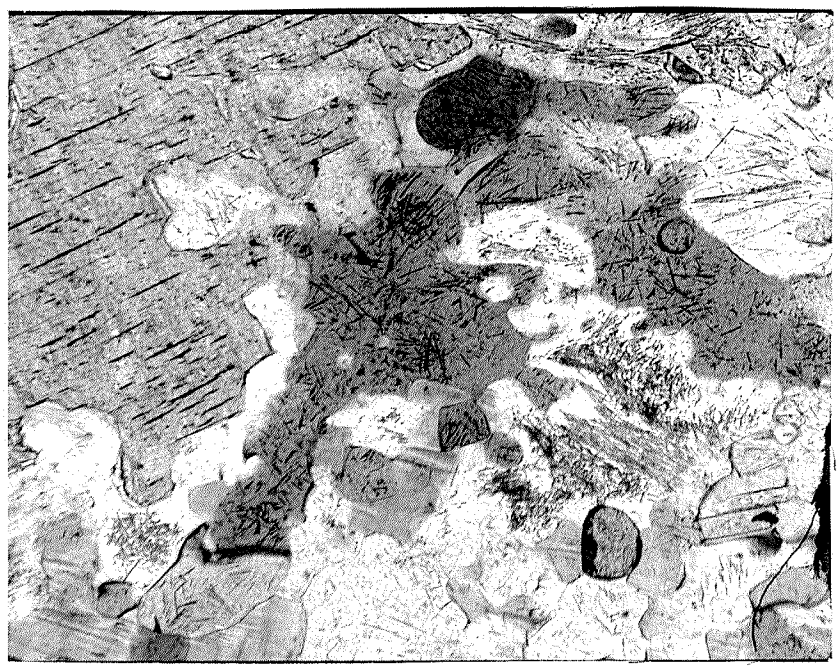

Fig. 15d. Muscovite and sillimanite bearing quartz in typical knot. Note clear quartz rim in contact with muscovite. Crossed polars.

enrichment in the surrounding matrix. Biotite and magnetite, the only mafic minerals present occur as less than 1 percent poikiloblasts within the knots but these same minerals constitute 15 and 5 percent respectively of the matrix. Plagioclase (An=20) content is low in the knots while its average content in the matrix is 16 percent. Muscovite is poikilitic, containing small anhedral grains of quartz and, less commonly, microcline and sillimanite. All minerals in the knots appear to be in equilibrium, and little evidence for reaction was found (except Fig. 14), even in the rare cases where muscovite, quartz, microcline and sillimanite co-exist in contact. The occurrence of reddish hematite staining (which is not a weathering product) along the 001 cleavage of muscovite in the knots is quite outstanding, since magnetite is the iron-oxide present not only in the matrix, but in all other Sickle-type rocks.

The matrix of the nodule-bearing rocks (Fig. 17) consists of a weakly-foliated, fine-grained, anhedral, equigranular mosaic of quartz, microcline, plagioclase, biotite and muscovite, all of which show a weak elongation parallel to foliation. Sillimanite was not present in the matrix of any of the thin sections studied.

Most muscovite in the matrix is aligned parallel to the dominant (biotite) foliation, but there is also a weak secondary (cross) foliation (Fig. 17). The muscovite present in the knots is aligned in this cross-orientation,

Fig. 16. Warped muscovite in typical knot. Crossed polars. Warping is taken as being indicative of a low-pressure environment.

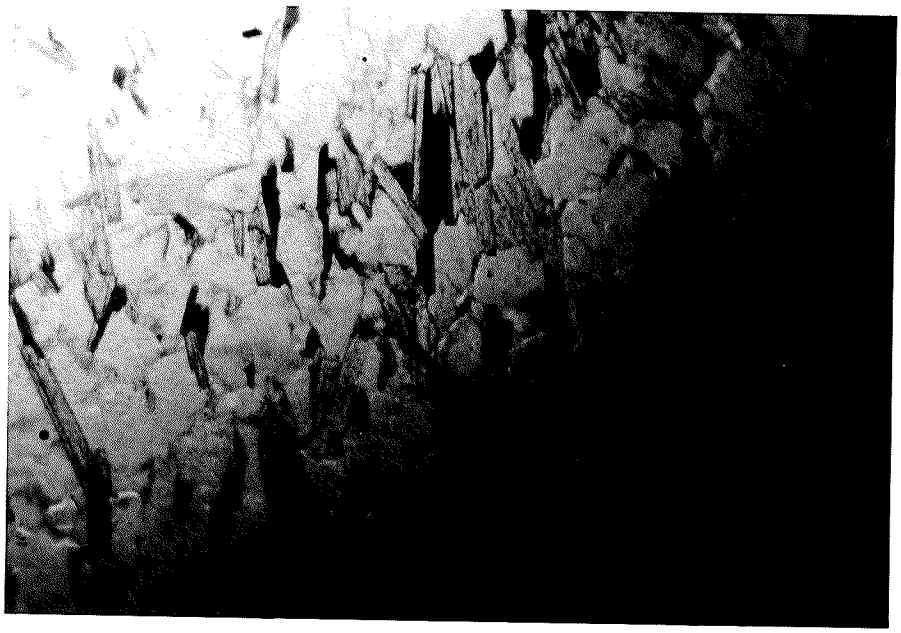

Fig. 17a. Typical matrix showing weak muscovite cross-foliation. Plane-polarized light.

Fig. 17b. Typical matrix exhibiting scattered muscovite grains in cross-orientation. Crossed polars.

and thus must have formed during the later event which yielded the cross-foliation (Fig. 16).

Apatite grain size in the nodules is coarser than in the surrounding matrix, indicating that apatite recrystallization must have occurred in the nodules.

Chemical Composition of Knots

Chemical and mesonormative compositions of typical nodule-bearing rocks, as well as representative nodule and matrix compositions, are listed in Tables III and IV.

The knots are richer in SiO_2 than the matrix by approximately 1 percent, and the mesonorms show a corresponding 3-4 percent quartz enrichment. As would be expected for such a small SiO_2 difference, actual quartz contents of knots and matrix are within 2-4 percent. However, quartz contents are greater in the matrix than in the knots (see Table II) which is the reverse of what one could expect from the chemical compositions. This discrepancy between mineral mode contents and predicted contents from chemical analyses is probably the result of highly variable knot composition and coarse grain size of the knots, which make accurate point counting difficult.

Alumina shows both positive and negative variations amounting to 1 percent or less, and therefore alumina migration, at least between knots and matrix, appears to be insignificant.

Table III

Chemical compositions of nodule-bearing rocks, nodules and matrix

Sample Identification*	T_1 Knots	T_1 Matrix	T_1 Composite (Actual)	T_1 Composite (Averaged)	T_{12} Knots	T_{12} Matrix	T_{12} Composite (Averaged)	T_3 Knots + Matrix	Milligan (1960) Knots
SiO_2	70.30	69.60	70.60	69.90	71.90	70.15	71.03	72.40	77.20
Al_2O_3	16.5	15.5	14.95	16.0	17.2	17.35	17.28	15.45	13.29
TiO_2	.33	.40	.36	.37	.23	.37	.30	.39	.26
Fe_2O_3	2.42	2.78	2.54	2.60	2.15	2.72	2.44	2.85	1.88
FeO	.36	.65	.71	.51	.36	.57	.47	.61	.32
MnO	.03	.05	.05	.04	.03	.05	.04	.04	.01
MgO	.85	1.57	1.44	1.41	.67	1.05	.86	1.00	.43
CaO	.44	.86	.80	.65	.17	0.56	.37	.15	.26
Na_2O	.98	1.60	1.50	1.29	.98	2.05	1.52	1.43	.61
K_2O	4.86	4.96	4.55	4.91	4.30	4.26	4.28	4.05	4.40
P_2O_5	.15	.09	.12	.12	.08	.07	.07	.08	.04
H_2O	2.05	1.48	1.56	1.77	1.74	.90	1.32	1.53	1.39
CO_2	.33	.35	.43	.34	.35	.32	.33	Nil	
	99.60	99.50	99.60		100.15	100.40			
Total Fe as Fe_2O_3	2.82	3.50	3.32	3.16	2.55	3.35	2.95	3.52	

* Sample locations are shown in Fig. 2.

Table IV

Mesonormative compositions of nodule-bearing rocks, nodules, and matrix.*

	T_1 Knots	T_1 Matrix	T_1 Composite	T_{12} Knots	T_{12} Matrix	T_{12} Composite	T_3 Composite
Apatite	.29	.18	.29	.15	.14	.14	.16
Pyrite							
Serpentine							
Ilmenite							
Albite	8.05	13.45	12.48	8.12	17.75	12.94	12.21
Orthoclase	24.48	14.05	21.84	22.04	21.95	22.00	20.57
Riebecite							
Magnetite	.83	1.41	1.64	.84	1.39	1.26	1.44
Anorthite	1.10	3.17	2.77	.30	2.24	1.32	.21
Corundum	9.18	6.04	6.54	10.91	8.97	9.81	8.97
Biotite	3.58	6.76	6.14	2.85	4.66	4.02	4.38
Diopside							
Hornblende							
Wollastinite							
Hypersthene							
Olvine							
Nepheline							
Hematite	.99	.87	.55	.83	.90	.86	.93
Spinel							
Quartz	38.56	34.50	37.07	42.45	36.59	38.51	42.75
Cation Used	87.04	92.17	89.31	88.49	94.60	90.86	91.62

* based on chemical compositions from Table III and calculated as in Barth, 1962. Sample locations are shown in Fig. 2.

TiO_2, Fe_2O_3, FeO, MnO and MgO contents are considerably smaller in the knots than in the matrix, reflecting the leucocratic nature of the knots (Table II). CaO and Na_2O contents of the nodules generally are smaller by half than those in the matrix. Actual and mesonormative mineralogical compositions, shown in Tables II and IV, reveal these deficiencies to be largely the result of the absence of plagioclase (An=20) in the knots.

K_2O contents of the nodules and matrix show small positive and negative deviations which are taken to indicate that K_2O migration, at least between nodule and matrix has been relatively insignificant. This may not have been the case, however, as will be discussed in the section dealing with "Possible Origins for the Knots".

P_2O_5 contents of the knots are slightly greater than in the surrounding matrix. Apatite is present as an accessory mineral in both the knots and matrix; visual estimates reveal these apatite contents to be somewhat higher in the knots than in the matrix. Migration of P_2O_5 from matrix to nodule or a simple reduction in nodule volume (i.e. by the expulsion of biotite, plagioclase and potash) are possible explanations for the higher P_2O_5 contents of the nodules

H_2O contents of the knots are 1.5 times those of the matrix. Muscovite and biotite in varying proportions are the two hydrous minerals present. Total values of muscovite

+ biotite in the knots, which are nearly three times those in the matrix, explain the difference in H_2O distribution.

INTERPRETATION OF METAMORPHIC MINERAL ASSEMBLAGES PRESENT

Methods of graphical analysis of metamorphic mineral assemblages were proposed by Thompson (1957 and 1961). Thompson's (1957) method involves neglecting H_2O and SiO_2; SiO_2 is assumed to be present in excess to form quartz. Mineral compositions within the tetrahedron Al_2O_3-K_2O-FeO-MgO are projected through the point for muscovite, KAl_3O_5, which is thereby present. Similar projections can be constructed for the system K_2O-Na_2O-Al_2O_3-SiO_2-H_2O. Figures 18 and 19 represent the various mineral assemblages given by Thompson as being characteristic of the sillimanite zone.

The following are possible interpretations of the metamorphic environment for formation of the knots.

A first hypothesis, with regard to metamorphic assemblages in the system SiO_2-Al_2O_3-MgO-FeO-K_2O-H_2O (Fig. 18), Sickle-type rocks have a bulk composition falling within the two phase region biotite-K-feldspar (plus quartz and muscovite). Hence, the formation of cordierite, andalusite, kyanite and sillimanite is prevented by the restriction of the chemical compositions. However, formation of such minerals is possible for Wasekwan-type rocks. Similarly, since the bulk composition of the Sickle-type

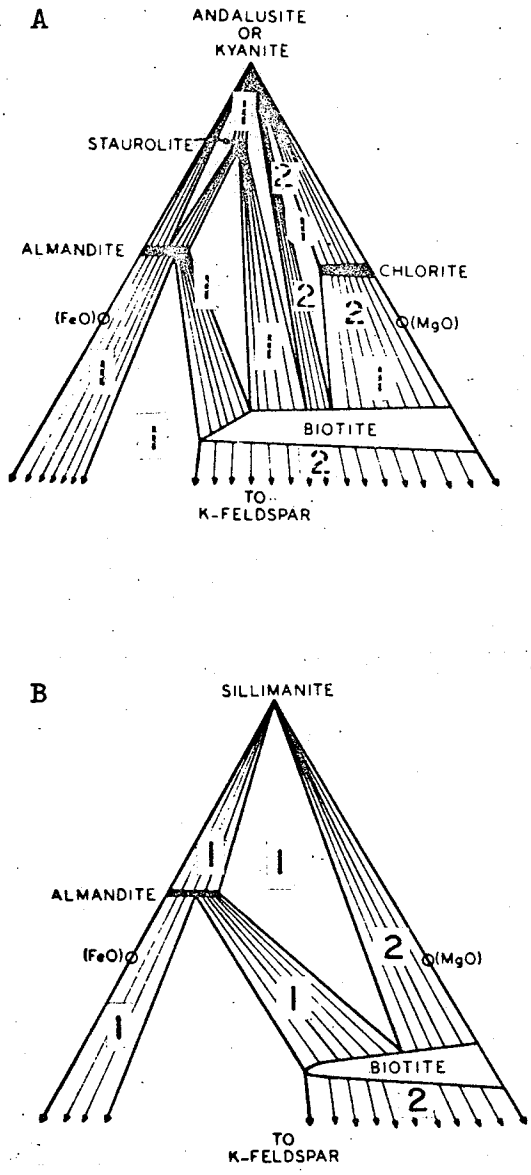

Fig. 18. Alumino-silicate bearing mineral assemblages for the amphibolite facies (coexisting with quartz and muscovite) in the system SiO_2 - Al_2O_3 - MgO - FeO - K_2O - H_2O (after Thompson 1957 and 1961). Metamorphic grade increases A to B.
(1) - indicates assemblage fields for Wasekwan rocks.
(2) - indicates assemblage fields for Sickle rocks.
Dashed numbers are used for assemblages not actually encountered but which would be expected at lower metamorphic grade.

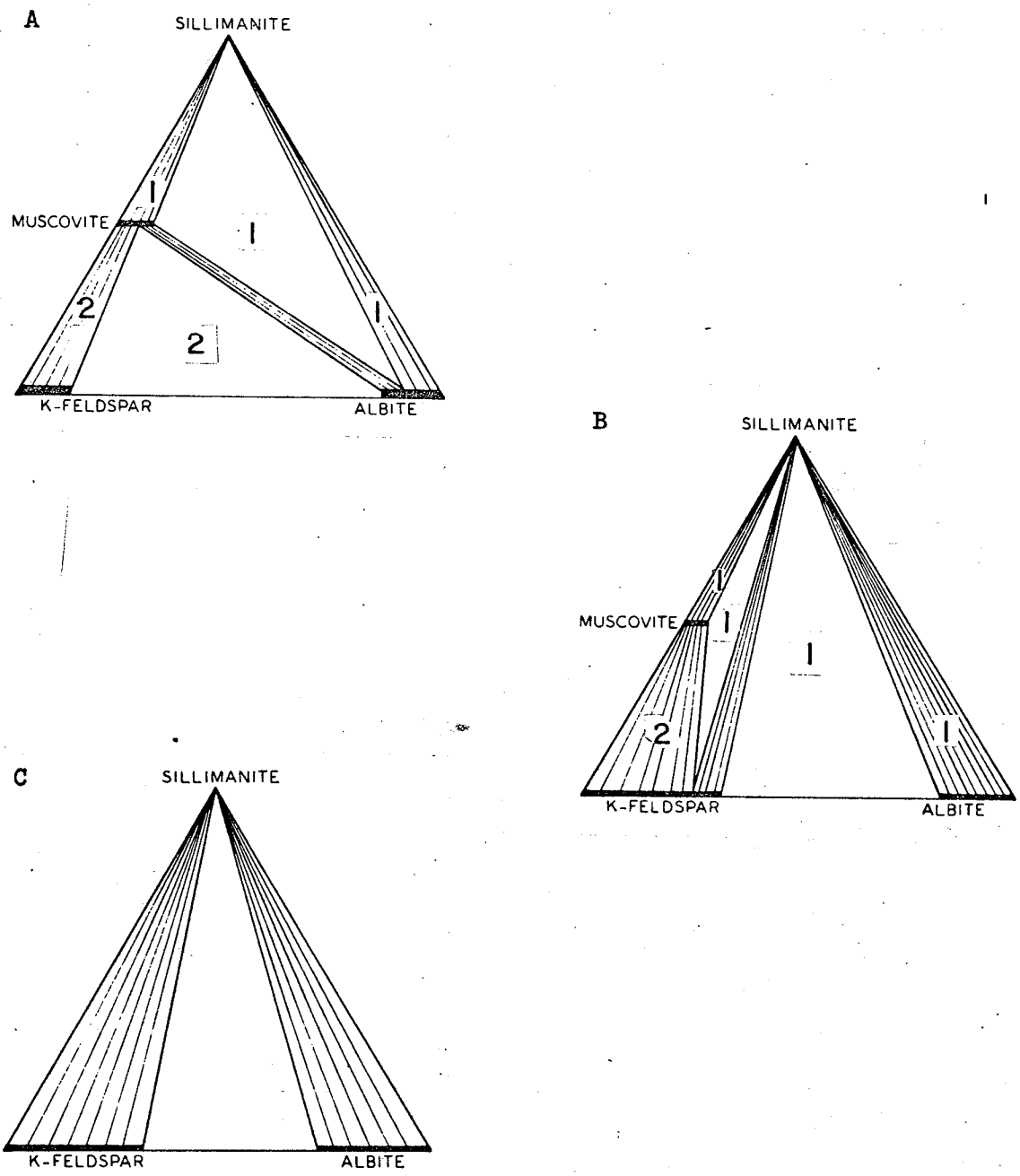

Fig. 19. Sillimanite bearing mineral assemblages for the amphibolite facies (coexisting with quartz and muscovite) in the system K_2O - Na_2O - Al_2O_3 - SiO_2 - H_2O (after Thompson, 1957 and 1961) ... increasing metamorphic grade from A to C.
(1) - indicates assemblage fields for knots.
(2) - indicates assemblage fields for matrix.

rocks (also the matrix of knot-bearing Sickle rocks) lies in the muscovite-K-feldspar-albite triangle of system K_2O-Na_2O-Al_2O_3-SiO_2-H_2O (Fig. 19a), sillimanite cannot stably co-exist with K-feldspar. D.A. Cranstone (1968) has attributed the formation of microcline-deficient quartz-muscovite-sillimanite knots in the Watt Lake area of the Lynn Lake district to conditions which favor tie-lines as shown in Fig. 19a. However, nodules in the Southern Indian Lake area and those found by Barry (1965) in the Granville Lake area, contain between 5 and 10 percent microcline, which co-exists with quartz, muscovite and sillimanite. Co-existing microcline and sillimanite (Figs. 19b and 19c) require somewhat higher metamorphic grade.

A second hypothesis, based on presence of sillimanite needles in direct contact with microcline, is that muscovite and quartz in the knots have reacted, at least in part, to yield sillimanite and microcline according to the reaction:

$$\underset{\text{muscovite}}{KAl_2AlSi_3O_{10}(OH)_2} + \underset{\text{quartz}}{SiO_2} \rightarrow \underset{\text{sillimanite}}{Al_2SiO_5} + \underset{\text{K-feldspar}}{KAlSi_3O_8} + \underset{\text{water}}{H_2O} \quad (1)$$

Lack of sillimanite in the matrix and the presence, in the knots, of quartz, muscovite, plagioclase, microcline and sillimanite, suggest that conditions of formation were those of the univariant reaction which related the assemblages shown in Figs. 19a and 19b. The restriction of sillimanite to the knots can best be explained by having the nodules act

as centers of reaction.

A third hypothesis of origin is that the assemblages present represent the products of Figs. 19b or 19c, which have in part undergone retrograde metamorphism. Thus all sillimanite originally present in the matrix would have reacted with potash feldspar according to reaction (1) above. Sillimanite in the knots would be protected (armoured) from reaction by the relatively coarse grain size and a lack of close grain to grain contact of the reactants. Sillimanite, other than the microscopic needles found in quartz, muscovite and rare microcline grains, is rare in the knots. Muscovite in the knots is apparently secondary in origin and grows in a cross orientation to the foliation in the surrounding rocks. However, reaction textures were not apparent even in the few cases where sillimanite and microcline grains were in mutual contact. Because of this lack of reaction textures it would appear that the above prograde reaction seems more likely than the retrograde reaction proposed here.

POSSIBLE ORIGINS FOR THE KNOTS

Losert (1968) has suggested that dealkalization, the removal of alkalis, from certain volumes of host rock would bring about a local excess of alumina and silica. Figure 20 exhibits potash deficient rims on granitic pebbles suggesting that a dealkalization process may have been active. If local dealkalization took place under the conditions of the sillimanite stability field, sillimanite would originate in the dealkalized volumes of the host rock. Dealkalization being controlled by anistropies such as bedding foliation and metamorphic layering would not affect the whole volume of the host rock. Sillimanite would, therefore, not be uniformly scattered throughout the rock. In contrast to the quartz-sillimanite nodules described by Losert (1968) nodules in the Southern Indian Lake area contain considerable microcline and abundant muscovite. The presence of these minerals in the knots may be explained by a second stage involving potash realkalization (but not Na_2O realkalization, see Table III). Microcline crystallization and muscovite formation (after sillimanite) in the knots would have occurred in this stage. The presence of quartz in poikiloblastic microcline (Fig. 15c) and microcline in poikiloblastic muscovite (Figs. 14 and 15d) as

Fig. 20. Light-coloured reaction rims on pebbles in Sickle-type conglomerate, where Potash feldspar has been removed. Area of thesis study east of Strawberry Island.

well as the general absence of sillimanite in muscovite support this hypothesis. If such a dealkalization-realkalization process had been active, biotite, magnetite and plagioclase should be concentrated in the knots, or, at least be present in equal proportion in knots and matrix. However, such minerals (and associated oxides,Table IV) have been deple ted in the knots suggesting that some other process of formation, perhaps a modified form of this dealkalization-realkalization must be appealed to.

Losert (1968) also gives a list of origins proposed by various authors. Those which might be applicable in the Southern Indian area are reviewed briefly.

The quartz-sillimanite knots are near spherical, and hence are late or post-tectonic in origin. Therefore, no origin which calls for primary structures is suitable.

Gradual feldspathization of quartz-sillimanite bands has been proposed by Sanders(1954). While K-feldspathization would explain the destruction of sillimanite in the matrix of nodule-bearing rocks, such a process does not seem probable because potash-feldspar distribution and average contents of Sickle-type rocks appear to be too uniform. That the reverse process was active, to a minor degree, is shown by leached, potash-feldspar-deficient rims, on some pebbles in the conglomerates found in the thesis area (Fig. 20).

Crystallizations of siliceous magma originating from

dissolution and melting of quartzites has been suggested by Brogger (1933). Such a process would appear feasible, especially since increasing knot size accompanies increasing anatexis of the host sandstone-arkose. It is thus possible that nodule formation was during the period of maximum temperature, which would have been subsequent to the final northeast tectonic event. During this period such siliceous magmas would be most likely to form and migrate. Many of the other processes suggested, however, would also be most active at a culmination of temperature.

Primary metamorphic differentiation in beds of suitable composition is a possible origin. In this process muscovite-quartz knots presumably are formed by segregation during increasing metamorphism. Such nodules were described by Milligan (1960) at Tod Lake, Manitoba, and by D.A. Cranstone (1968) at Watt Lake (east), Manitoba. The presence of sillimanite and the absence of potash-feldspar in knots from these areas indicates that reaction between quartz and muscovite to yield potash-feldspar did not occur. With increasing metamorphic grade quartz and muscovite in the nodules would react upon reaching the appropriate temperature pressure conditions. This is apparently the case for K-feldspar-bearing knots found in the Southern Indian Lake area. Similar potash-feldspar-bearing nodules have been noted by Barry (1965) and Godard (1966) in the Trophy Lake and Watt Lake (west) areas respectively.

CONCLUSIONS

Metamorphic grade reached during the first period of folding (intense, isoclinal) is uncertain, however, extensive recrystallization and possible sillimanite formation occurred. The metamorphic grade reached during a second period of deformation (north-east trending) was the upper amphibolite facies of the low or medium (cordierite-bearing) pressure facies series.

Quartz-muscovite-microcline-plagioclase-sillimanite knots in the Southern Indian Lake area are probably the product of simple metamorphic segregation during cordierite-amphibolite grade metamorphism or, may have been formed by potash realkalization of quartz-sillimanite knots formed in an earlier dealkalization event. Quartz-muscovite-sillimanite knots occurring elsewhere in the Lynn Lake District appear to have formed by similar processes but at somewhat lower metamorphic grade.

The relatively undeformed nature of such knots and the weak muscovite cross-foliation common to knots and matrix, indicates nodule formation must have been extremely late in the tectonic history of the area. The northeasterly orientation of this cross-foliation is coincident with an average northeasterly plunge of elongated knots; these

structures are parallel to the final axis of regional folding, and are an indication of formation very late in this tectonic event.

LIST OF REFERENCES

Barry, G.S. 1965. Geology of the Trophy Lake Area (East Half). *Man. Mines Br.*, Publ. 63-3.

Barth, T.F.W. 1962. Theoretical Petrology (2nd Edition). J. Wiley & Sons, New York, London, pp. 337-343.

Brogger, W.C. 1933. On several archaean rocks from the south coast of Norway. I. Nodular granites from the environs of Kragero Skrift. Nork. Vedensk. *Ak. i. Oslo, Mat. Nt. Kl.*, vol. 8, pp. 1-97.

Cranstone, D.A. 1968. Geology of the Watt Lake Area. *Man. Mines Br.*, Publ. 61-5.

Cranstone, J.R. 1971. Geology of the Southern Indian Lake Area: Northern and Eastern Portions. *Man. Mines Br.*, Publ. 71-2-J.

Godard, J.D. 1966. Geology of the Watt Lake Area (West Half). *Man. Mines Br.*, Publ. 61-4.

Losert, Jiri 1968. On the genesis of nodular sillimanite rocks, *XXIII International Geological Congress*, vol. 4, pp. 109-122.

McInnes, W. 1913. The basins of the Nelson and Churchill Rivers. *Geol. Surv. Can.*, Mem. 30, pp. 84-86.

Milligan, G.C. 1960. Geology of the Lynn Lake district. *Man. Mines Br.*, Publ. 57-1.

Newton, R.C. 1966. Kyanite-andalusite equilibrium from 700° to 800°C.. *Science*, vol. 153, pp. 170-172.

Quinn, H.A. 1959. Big Sand Lake, Manitoba (marginal notes). *Geol. Surv. Can.*, Preliminary Series Map, 45-1959.

Richardson, S.W. 1968. Staurolite stability in part of the system Fe-Al-Si-O-H. *Jour. Petrol.*, vol. 9, Part 3, pp. 467-488.

Sanders, L.D. 1954. The status of sillimanite as an index of metamorphic grade in the Kenya Basement. *Geol. Mag.*, vol. 91, pp. 144-152.

Thompson, J.B., Jr. 1957. The graphic analysis of mineral assemblages in pelitic schists. *Amer. Min.*, vol. 42, pp. 842-858.

———— 1961. Mineral facies in pelitic schists. *In:* Fiziko-Khimicheskie Problemii Formerovaniya Garnyikh Porod i Rud (Physioco-chemical problems of the formation of rocks and ores), Sokolov, G.A., ed. (in Russian), *Acad. Nauk. U.S.S.R., Inst. Geo. Ore Deposits, Petrog., Mineral., Gerchem.*, pp. 313-324, English summary, pp. 323-324.

Turner, F.J. and Verhoogen, J. 1960. Igneous and Metamorphic Petrology (2nd Edition). McGraw-Hill, New York.

Tuttle, O.F. and Bowen, N.L. 1958. Origin of granite in light of experimental studies in the system $NaAlSi_3O_8$-SiO_2. *Geol. Soc. Amer.*, Mem. 74.

Winkler, H.G.F. 1965. Petrogenesis of Metamorphic Rocks. Springer Verlag, New York.

———— 1967. Petrogenesis of Metamorphic Rocks, Revised Second Edition. Springer Verlag, New York.

WASEKWAN TYPE ROCKS

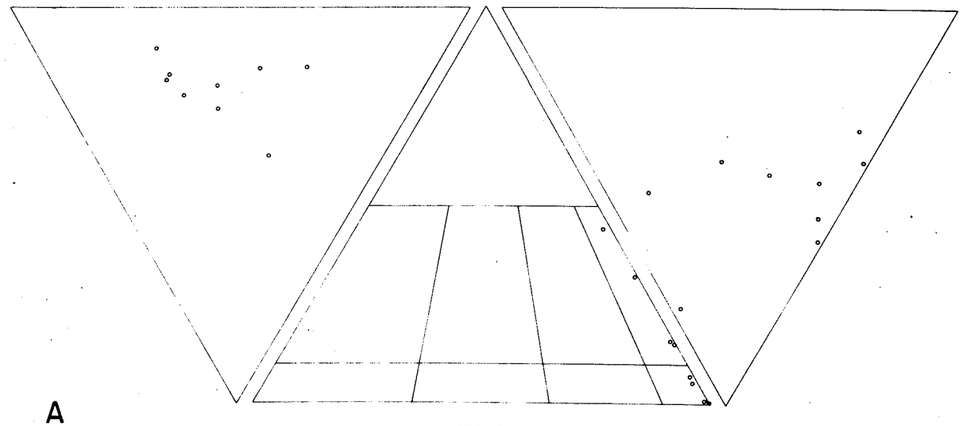

A

META-CALCAREOUS ROCKS 3

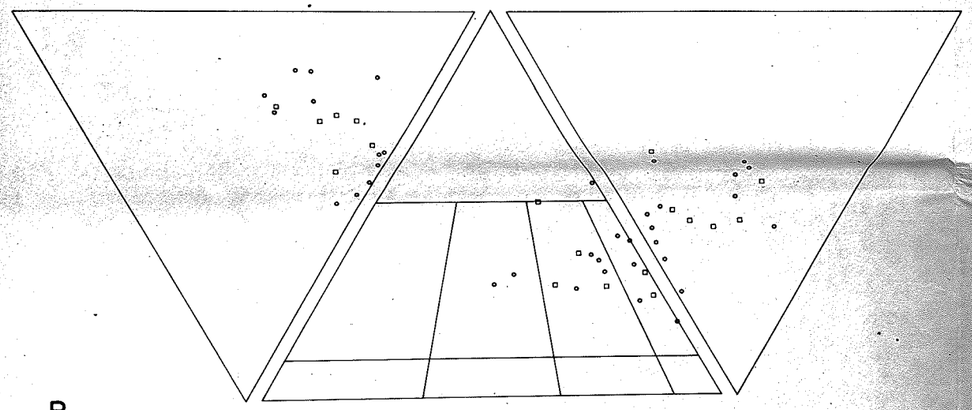

B

ANATECTIC GRANODIORITE I (6)

- Long Point
- Budgie Island, South of Bear Narrows

SICKLE TYPE ROCKS

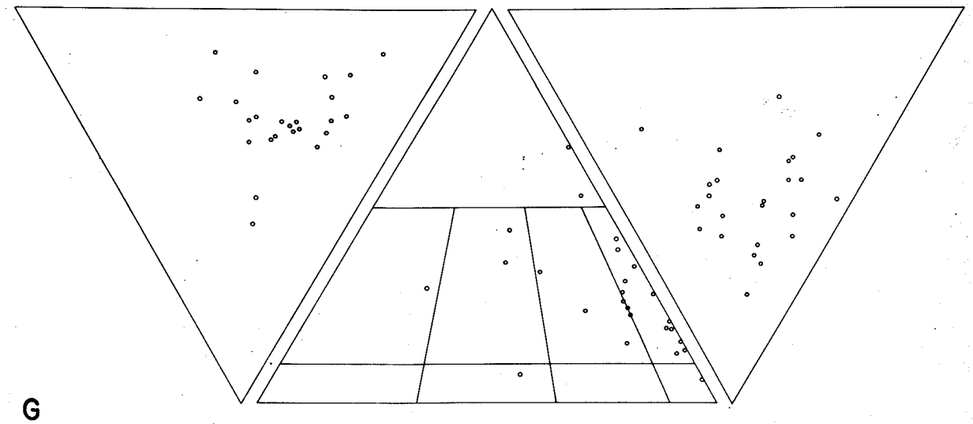

G

PLAGIOCLASE PARAGNEISS 8(1)

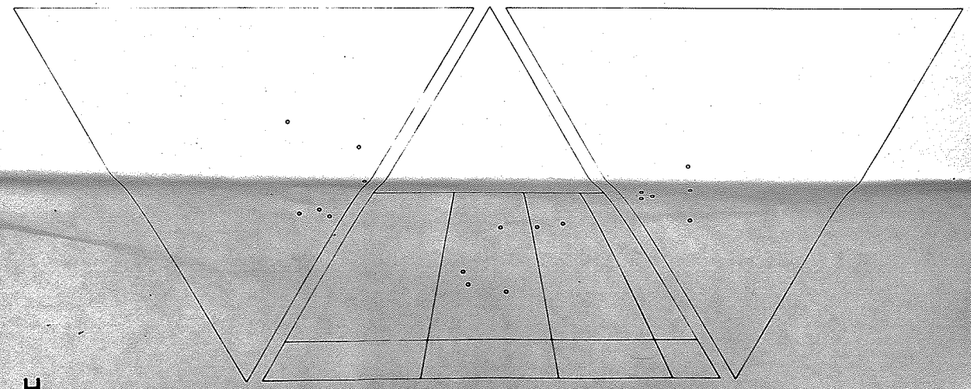

H

ANATECTIC QUARTZ MONZITE 7(4)

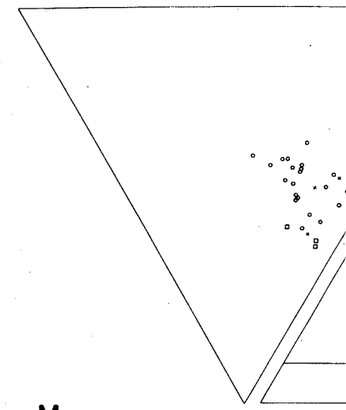

M

PORPHYRI

- Cousins
- Strowbe
- Loon Is

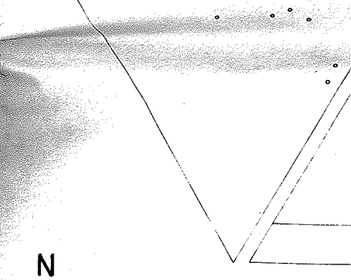

N

MEDIUM-GRAINE

- Salute Islar

GRANITIC INTRUSIVE ROCKS

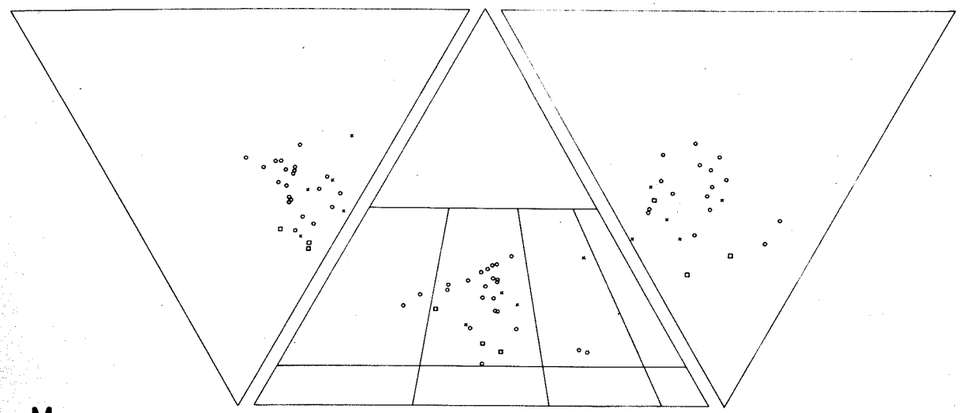

M

PORPHYRITIC BIOTITE QUARTZ MONZONITE 15

- o– Cousins Lake sheet
- x– Strowberry Island
- o– Loon Island

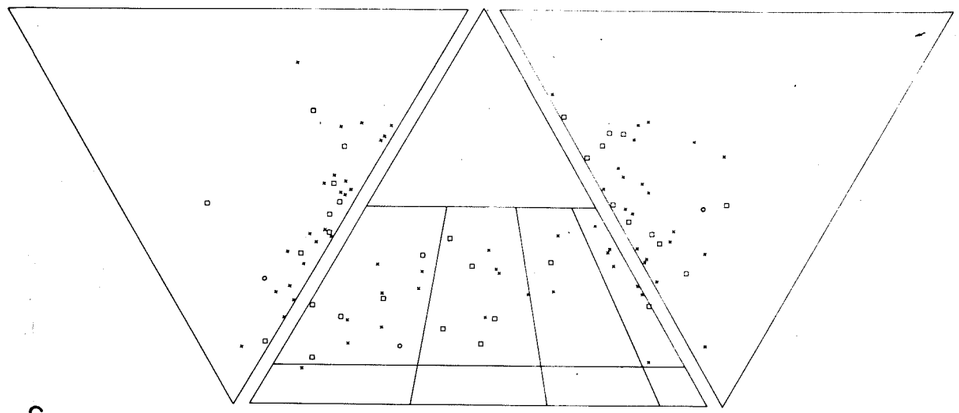

S

PEGMATITE 21

- □– for Sickle-type rocks
- x– for Wasekwan-type rocks
- o– for gabbros, probably derived from surrounding gneisses

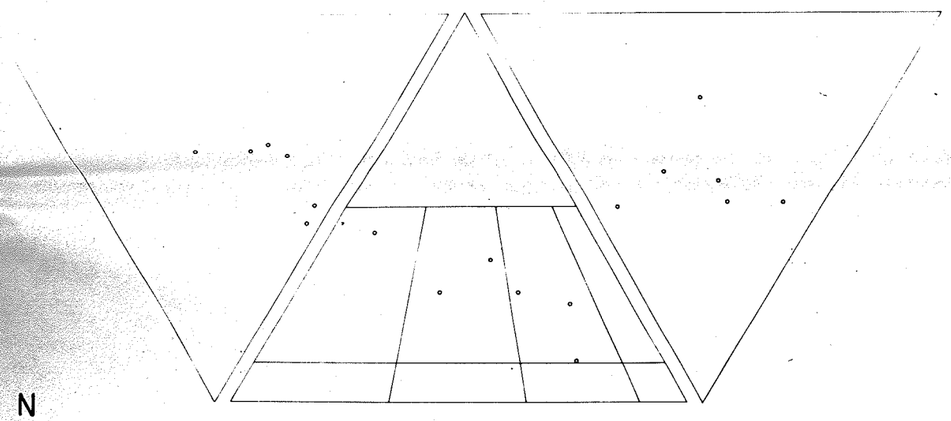

N

MEDIUM-GRAINED HORNBLENDE QUARTZ MONZONITE 14b

- o– Salute Island

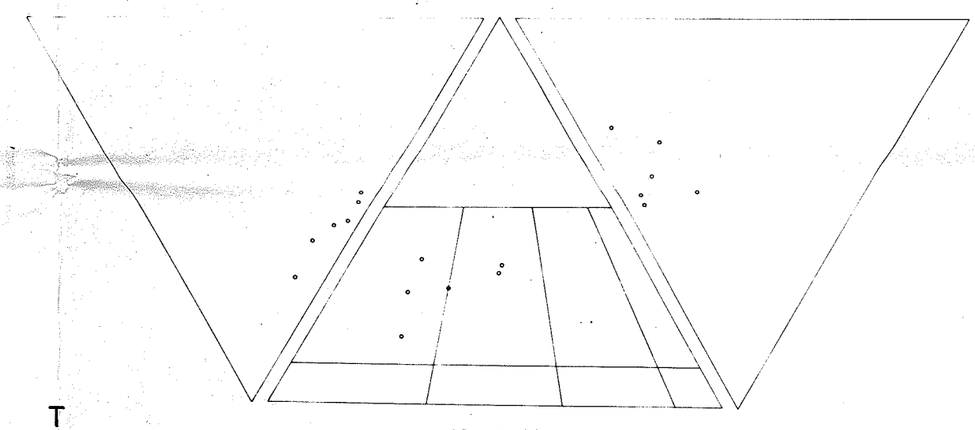

T

APLITE 20

□- Budgie Island, South of Bear Narrows

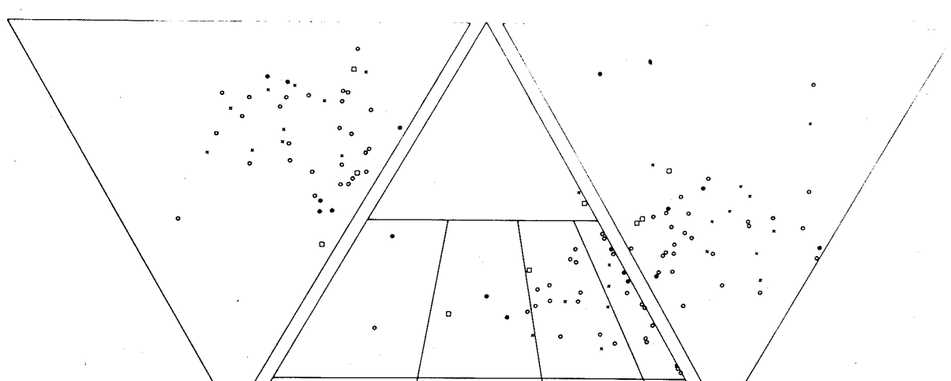

C

PLAGIOCLASE DIATEXITE I(4)

- o Missi area.
- • Nutter Lake.
- □ East of Turtle Island.
- · Long Point.

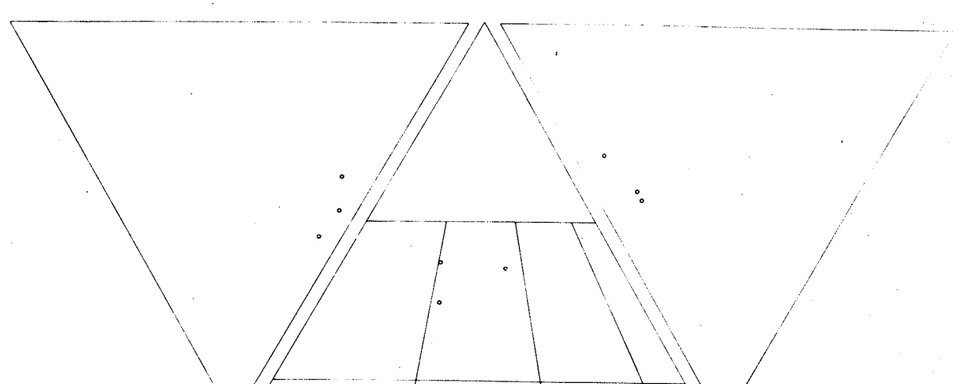

I

POTASSIUM FELDSPAR DIATEXITE 7(3)

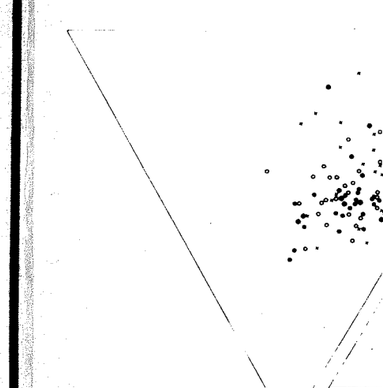

O

K

PORPHR

- •– Ho
- o N
- · To
- • Co

POST-SICKLE

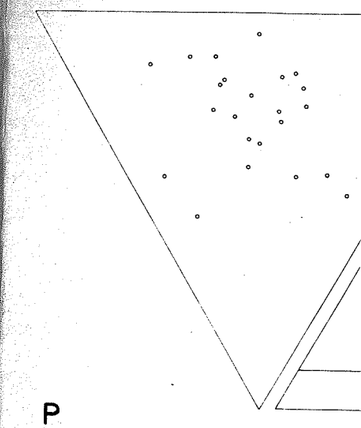

P

M

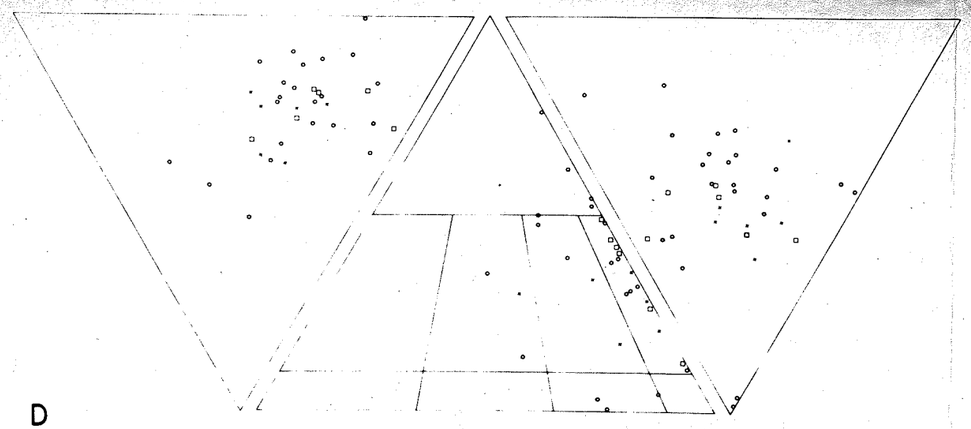

D

PLAGIOCLASE METATEXITE I(2)

- •– Nutter Lake sheet
- c– Missi Rapid sheet
- o– Torrance Lake sheet

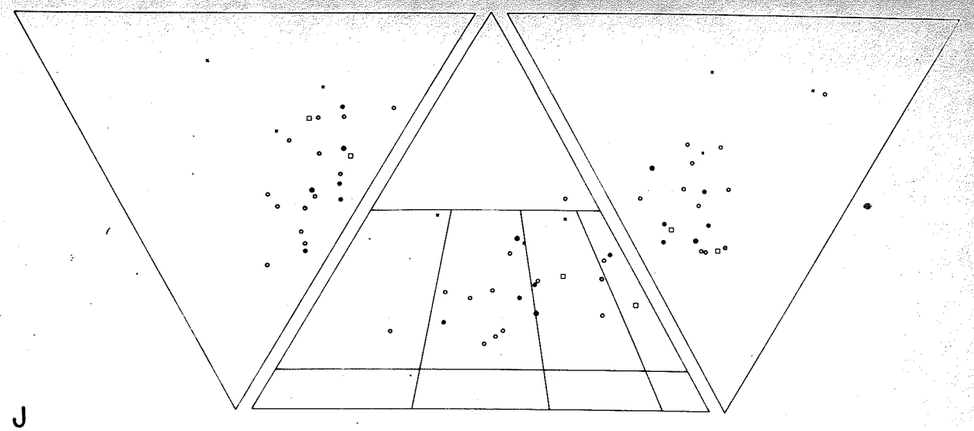

J

POTASH FELDSPAR METATEXITE 7(2)

- •– North of Missi Falls.
- □– West of Bean Narrows.
- o– Loon Narrows
- •– Inclusions in hornblende quartz monzonite South of Long Point.
- ·– Strawberry Island

South of Long Point

O

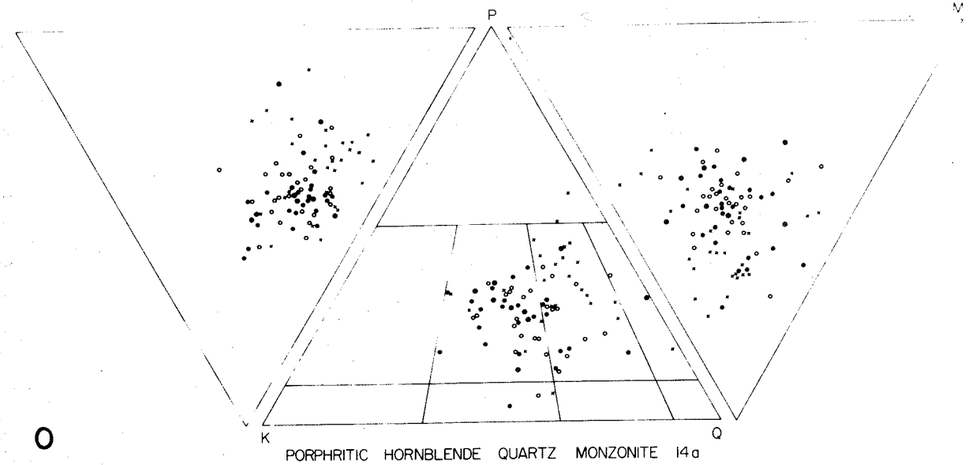

PORPHRITIC HORNBLENDE QUARTZ MONZONITE 14a

- ●– Hammond Point and Moss Lake sheets
- ○ Nutter Lake and Missi Rapid sheets
- · Torrance Lake sheet
- • Cousins Lake sheet

U

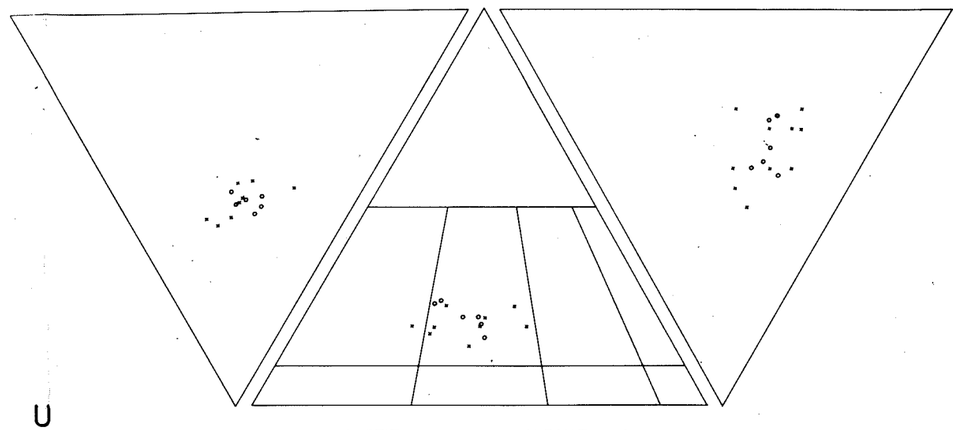

MAGNETITE QUARTZ MONZONITE 19

- ○– Hammond Point – Moss Lake 19b.
- ·– East of Sand Point. 19a.

POST-SICKLE TYPE BASIC INTRUSIVE ROCKS

P

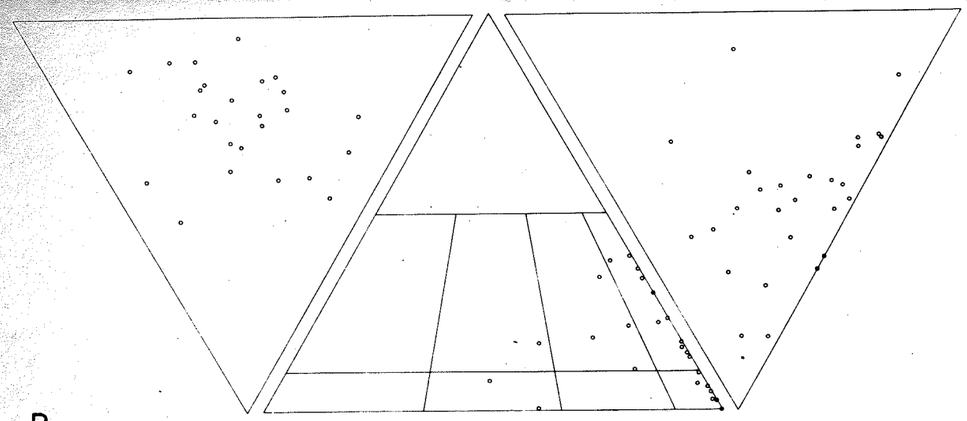

META-GABRO and META-DIORITE 10

V

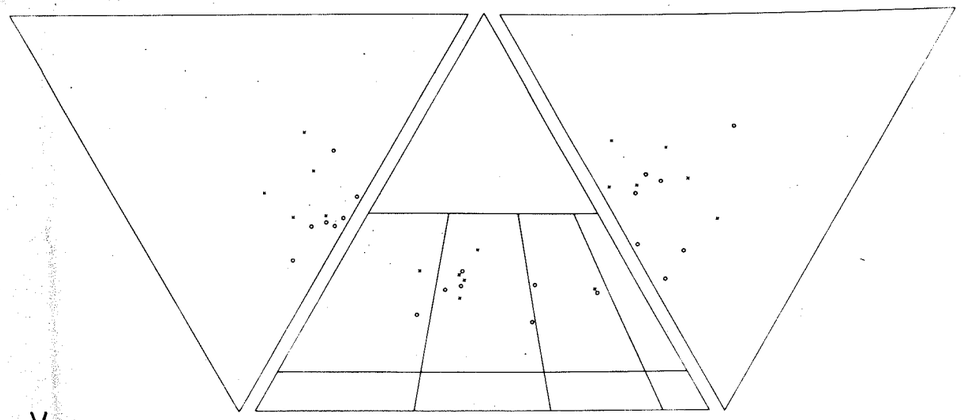

- ○-FINE-GRAINED QUARTZ MONZONITE 16
  - Sand Point Area
- ×-ANATECTIC OR INTRUSIVE QUARTZ MONZONITE 7(4)

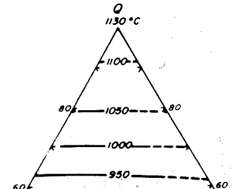

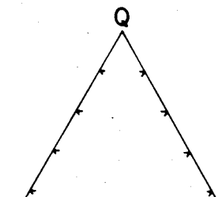

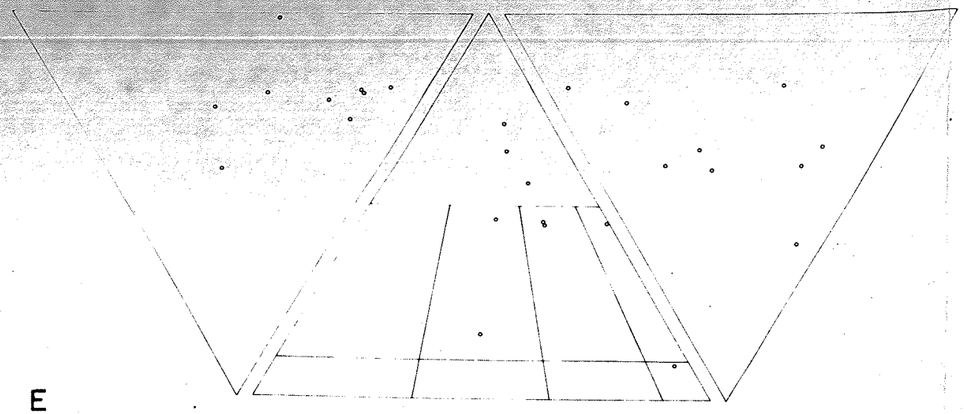

E

PLAGIOCLASE PARAGNEISS 1(1)

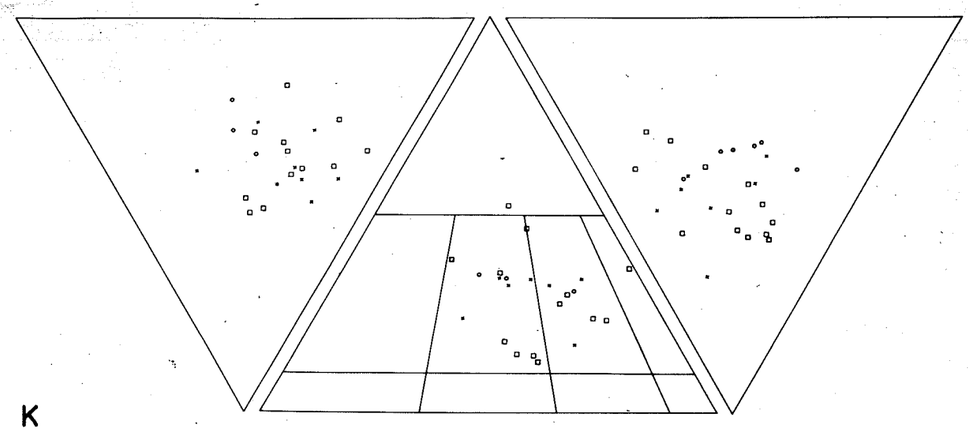

K

POTASSIUM FELDSPAR PARAGNEISS 7(1)

□ - Loon Narrows
× - Strawberry Island - Salute Island
○ - North of Missi Falls

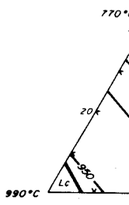

Q

Projection o
$NaAlSi_3O_8$-$KAlSi_3O_8$-H
marks the composition
tions are given in we
BOWEN, 1958, and from

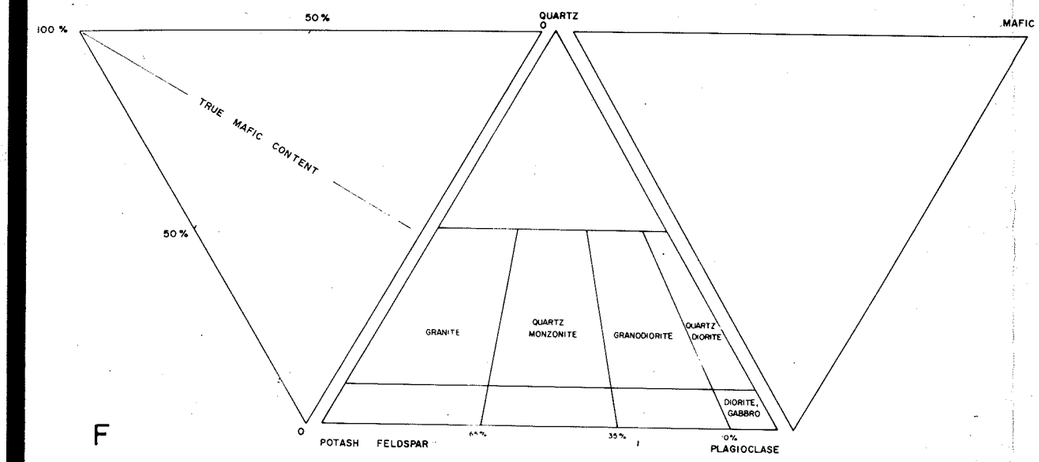

F

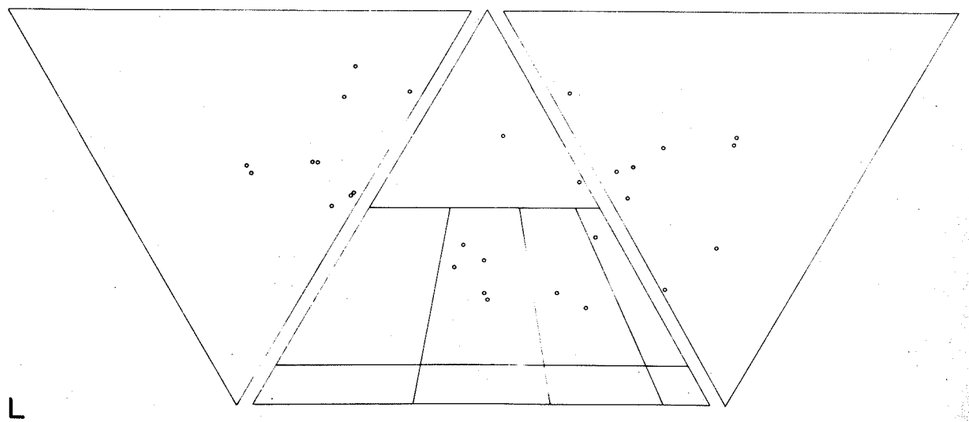

L

META-CONGLAMERATE (7a)

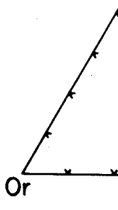

R

Or

Normative
systems and other ex
Dots = "minimum melt
ratio as given in Tabl
interpolated Ab/An ra
containing 0,05 m HCl
perature of "minimum
dashed line is shifte
granite compositions is

Figure. 8 Ternary plots (plagioclase-potash feldspar-quartz and plagioclase-quartz-mafic) versus true mafic content. Rock classification fields are after Bateman (1962). Ternary plots referring to anatectic and minimum melt compositions are from Winkler (1967).

South of Long Point

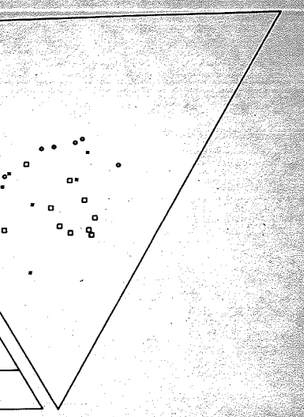

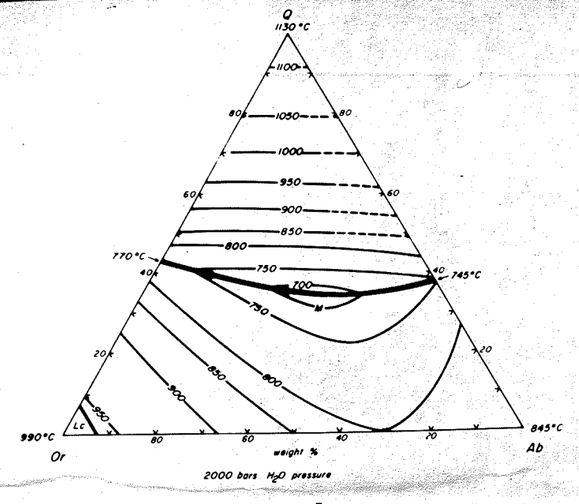

Projection of the isotherms and of the cotectic line of the system SiO_2-$NaAlSi_3O_8$-$KAlSi_3O_8$-H_2O at P_{H_2O} = 2000 bars. E_1 and E_2 are eutectic points; M marks the composition of the temperature minimum on the cotectic line. Compositions are given in weight percent (drawn on the basis of data from TUTTLE and BOWEN, 1958, and from H. R. SHAW, 1963, *Amer. Miner.*, 48, 883-896). Lc = leucite.

Q

W

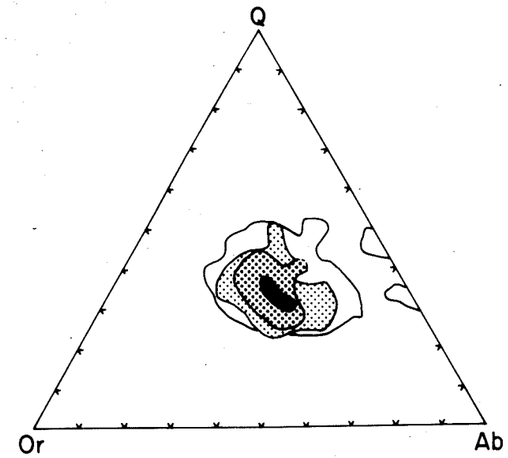

Frequency distribution of the normative Q:Ab:Or-ratios of 1190 granitic rocks (from WINKLER and von PLATEN, 1961, *Geochim. et Cosmochim. Acta*, 250 ff.). The fields bounded by the outermost line include 86% of all granites; the three patterned fields, 75%; the finely-stippled field and the black field, 53%; the black field alone includes 14%. The frequency maximum lies within the black field.

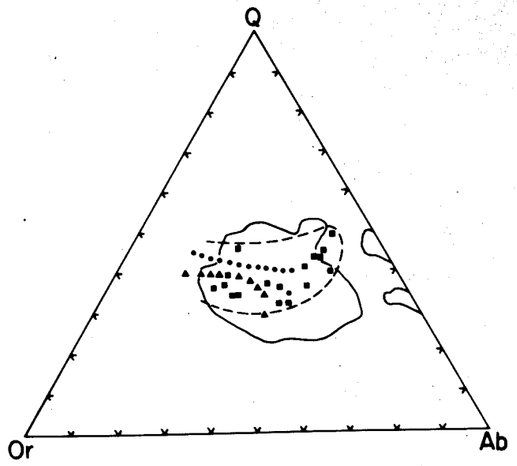

R

Normative Q:Ab:Or ratios of "minimum melt" compositions in granitic systems and other experimentally produced anatectic melts at P_{H_2O} = 2000 bars. Dots = "minimum melt" compositions in H_2O-saturated systems with various Ab/An ratio as given in Table 9. Circles = "minimum melt" compositions in systems with interpolated Ab/An ratio. Solid and open triangles = "minimum melt" in systems containing 0.05 m HCl (see Table 11). Diamonds = anatectic melts above the temperature of "minimum melt." At pressure > 2000 bars, the field bounded by the dashed line is shifted toward the Ab corner. The solid line showing the field of granite compositions is taken from Figure

X

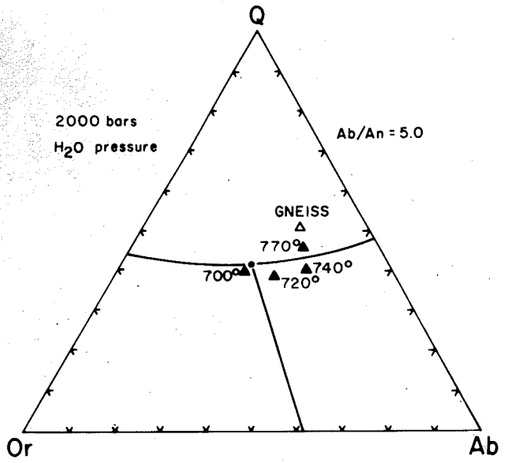

Anatexis of a quartz-plagioclase-cordierite-K-feldspar-biotite-sillimanite paragneiss derived from greywacke. Increasing temperature changes the ratio, Q:Ab:Or, in the anatectic melts. Composition of melts is shown at 700°C (slightly above the temperature of the beginning of melting), at 720°C, 740°C, and 770°C. The position of the cotectic lines is shown for the Q-Ab-An-Or-H_2O system at P_{H_2O} = 2000 bars and having an Ab/An ratio of 5.0.